GLADA Report 5

Global Assessment of Land Degradation and Improvement

1. Identification by remote sensing

Z G Bai

D L Dent

L Olsson

M E Schaepman

LADA

Land Degradation Assessment in Drylands

ISRIC World Soil Information

FOOD AND AGRICULTURE ORGANIZATION OF THE UNITED NATIONS

FIAT PANIS

Citation:

Bai ZG, Dent DL, Olsson L and Schaepman ME 2008. *Global assessment of land degradation and improvement 1: identification by remote sensing*. Report 2008/01, FAO/ISRIC – Rome/Wageningen

PRELIMINARY FINDINGS

1. **Land degradation is a global environment and development issue.** Up-to-date, quantitative information is needed to support policy and action for food and water security, economic development, environmental integrity and resource conservation. To meet this need, the Global Assessment of Land Degradation and Improvement (GLADA) uses remote sensing to identify degrading areas and areas where degradation has been arrested or reversed. Within the parent LADA program, this screening will be followed up by field investigations to establish the situation on the ground.

2. **Land degradation is defined as a long-term decline in ecosystem function and productivity and measured in terms of net primary productivity.** The remotely-sensed normalized difference vegetation index (NDVI) is used as a proxy; its deviation from the norm may serve as an indicator of land degradation and improvement if other factors that may be responsible (climate, soil, terrain and land use) are accounted for. Rainfall effects may be accounted for by rain-use efficiency (NDVI per unit of rainfall) and residual trends of NDVI, temperature effects by energy-use efficiency (derived from annual accumulated temperature). Translation of NDVI in terms of net primary productivity enables economic appraisal; land degradation is indicated by a declining trend of climate-adjusted net primary productivity and land improvement by an increasing trend.

3. **Land degradation is cumulative – this is the global issue.** The 1991 GLASOD assessment indicated that 15 per cent of the land surface was degraded; the 24 per cent identified by the present assessment hardly overlaps. This implies that land degradation over the past 23 years has mainly affected new areas; while some areas of historical land degradation have been so severely affected that they are now stable at stubbornly low levels of productivity.

4. **Analysis of 23-year GIMMS NDVI data reveals a declining trend across some 24 per cent of the global land area.** Spatial patterns and temporal trends of NDVI and rain-use efficiency are analysed for the period 1981-2003 at 8km resolution. Degrading areas are mainly in Africa south of the Equator, SE Asia and S China, N-Central Australia, the Pampas, and swaths of boreal forest in Siberian and N America.

5. **Almost 20 per cent of degrading land is cropland - more than 20 per cent of all cultivated areas**; 24 per cent is broadleaved forest, 19 per cent needle-leaved forests, 20-25 per cent rangeland. Cropland occupies only 12 per cent of the land area, so degradation is over-represented in cropland globally.

6. **Some 16 per cent of the land area shows an increase in climate-adjusted net primary productivity.** 18 per cent of the improving land is cropland (20 per cent of the total croplands), 23 per cent is forest and 43 per cent rangeland.

7. **There is only a weak correlation with biophysical factors other than land cover**: 78 per cent of degrading land is in humid regions, 8 per cent in the dry sub-humid, 9 per cent in the semi-arid, and 5 per cent in arid and hyper-arid regions. There is no obvious relationship between degrading land and the nature of soil or terrain – degradation is driven mainly by management.

8. **About 1.5 billion people depend directly on the degrading areas.** There is a weak correlation between degrading land and rural population density but more detailed analysis of land use history is needed to tease out the underlying social and economic drivers.

Key words: land degradation/improvement, remote sensing, NDVI, net primary productivity, land use/cover, global relationships

Contents

Figures

Tables

Abbreviations

AVHRR	Advanced Very High Resolution Radiometer
Biome-BGC	Biome-BioGeochemical Cycles, Terrestrial Ecosystem Process Model
CIAT	International Centre for Tropical Agriculture, Cali, Columbia
CIESIN	Center for International Earth Science Information Network, Colombia University, Palisades, NY
CoV	Coefficient of Variation
CRU TS	Climate Research Unit, University of East Anglia, Time Series
ENSO	El Niño/Southern Oscillation
EUE	Energy-Use Efficiency
FAO	Food and Agriculture Organization of the United Nations, Rome
GEF	The Global Environment Facility, Washington DC
GIMMS	Global Inventory Modelling and Mapping Studies, University of Maryland
GLADA	Global Assessment of Land Degradation and Improvement
GLASOD	Global Assessment of Human-Induced Soil Degradation
GPCC	The Global Precipitation Climatology Centre, German Meteorological Service, Offenbach
HANTS	Harmonic Analyses of NDVI Time-Series
JRC	European Commission Joint Research Centre, Ispra, Italy
LADA	Land Degradation Assessment in Drylands
Landsat ETM+	Land Resources Satellite, Enhanced Thematic Mapper
MOD17A3	MODIS 8-Day Net Primary Productivity data set
MODIS	Moderate-Resolution Imaging Spectroradiometer
NDVI	Normalized Difference Vegetation Index
NPP	Net Primary Productivity
RESTREND	Residual Trends of sum NDVI
RUE	Rain-Use Efficiency
SOTER	Soil and Terrain database
SPOT	Système Pour l'Observation de la Terre
SRTM	Shuttle Radar Topography Mission
TRMM	The Tropical Rainfall Measuring Mission
UNCED	United Nations Conference on Environment and Development
UNEP	United Nations Environment Programme, Nairobi
VASClimO	Variability Analyses of Surface Climate Observations

1 Introduction

1.1 The need for a new assessment

Ever-more-pressing demands on the land from economic development, burgeoning cities, and growing rural populations are driving unprecedented land-use change. In turn, unsustainable land use is driving land degradation: a long-term loss in ecosystem function and productivity that requires progressively greater inputs to repair the situation. Its symptoms include soil erosion, nutrient depletion, salinity, water scarcity, pollution, disruption of biological cycles, and loss of biodiversity. This is a global development and environment issue recognised by the UN Convention to Combat Desertification, the Convention on Biodiversity, the Kyoto Protocol on Climatic Change, and the Millennium Goals (UNCED 1992, UNEP 2007).

Quantitative, up-to-date information is needed to support policy development for food and water security, environmental integrity, and economic development. But land degradation is a contentious field; crucial questions that must be answered in a scientifically justifiable way include: Is land degradation a global issue or a collection of local problems? Which regions are hardest hit; how hard are they hit? Is it mainly a problem of drylands? Is it mainly associated with farming? Is it related to population pressure - or poverty? This assessment within the FAO program *Land Degradation Assessment in Drylands (LADA),* addresses these questions using justifiable methods.

The only previous harmonized assessment, the *Global Assessment of Human-induced Soil Degradation (GLASOD)*, distinguished degrees of degradation and various kinds of land degradation, e.g. soil erosion by water or by wind, salinity, nutrient depletion (Oldeman and others 1991). GLASOD was a map of perceptions - not a measure - of land degradation and is now out-of-date; its qualitative judgments (Appendix Table S1) have proven inconsistent and hardly reproducible, relationships between land degradation and policy-pertinent criteria were unverified (Sonneveld and Dent 2007) - as its authors were the first to point out.

1.2 Indicators

Land degradation may be defined as a long-term loss of ecosystem function and productivity caused by disturbances from which the land cannot recover unaided. It may be measured by change in net primary productivity (NPP - the rate at which vegetation fixes CO_2 from the atmosphere less losses through respiration); deviation from the norm may be taken as an indicator of land degradation or improvement. As a proxy, the remotely sensed normalized difference vegetation index (NDVI) has been shown to be related to biophysical variables that control vegetation productivity and land/atmosphere fluxes (Hall and others 2006) such as: leaf-area index (Myeni and others 1997), the fraction of photosynthetically-active radiation absorbed by vegetation (Asrar and others 1984), and NPP (Alexandrov & Oikawa 1997, Rasmussen 1998a,b). It has also been used to estimate vegetation change, either as an index (Anyamba & Tucker 2005; Olsson and others 2005) or as one input to dynamic vegetation models (Nemani and others 2003; Seaquist and others 2003; Fensholt and others 2006); consistent time-series data at spatial resolutions from 20m to 8km (Brown and others 2006) enable analysis and generalization. This study uses NDVI data produced by the Global Inventory Modelling and Mapping Studies (GIMMS) group from measurements made by the AVHRR radiometer on board US National Oceanic and Atmospheric Administration satellites. The fortnightly images at 8km spatial resolution are corrected for calibration, view geometry, volcanic aerosols, and other effects not related to vegetation cover (Tucker and others 2004).

A negative trend in NDVI does not necessarily indicate land degradation, nor does a positive trend necessarily indicate land improvement. Biomass depends on several factors including: climate - especially fluctuations in rainfall, sunshine, and length of growing season; land use; large-scale ecosystem disturbances such as fires; and the global increase in nitrate deposition and atmospheric carbon dioxide. To interpret NDVI trends in terms of land degradation or improvement, we have to eliminate false alarms, in particular those arising from climatic variability and land use change. Globally, this can be done for climate, for which a century's consistent data are available, but global time series are not available for land use which has to be addressed case-by-case.

Where productivity is limited by rainfall, rain-use efficiency (RUE, the ratio of NPP to rainfall) accounts for variability of rainfall and, to some extent, local soil characteristics (Houérou 1984, Houérou and others 1988). The combination of satellite-based estimation of NDVI and station-observed rainfall has been used to assess land degradation at various scales (Holm and others 2003, Prince and others 2007) but RUE, itself, is strongly correlated with rainfall; in the short term, it says more about rainfall fluctuation than about land degradation but we judge that its long-term trends distinguish between the effects of rainfall and land degradation on NPP. To get around the correlation of RUE with rainfall, Wessels and others (2007) have suggested the alternative use of residual trends (RESTREND) – the difference between the observed NDVI and that predicted from the local rainfall-NDVI relationship. Both approaches are employed in this report.

There are caveats when applying these data globally:

1) The NDVI signal is sometimes saturated at closed vegetation canopy (Ripple 1985) so it is more sensitive for cropland and rangeland than for forest; however, it is still useful for forest;
2) Cloud screening was performed and maximum NDVI was read out for a composite of 15 days, but NDVI may still be underestimated for cloudy areas;
3) The great spatial variability of rainfall in drylands makes interpolation of point measurements problematic, and observation stations are sparse in many of these areas.

NDVI is simply a ratio of red and near-infrared light reflected by the land surface. To provide a more tangible measure of land degradation that is amenable to economic analysis, the GIMMS NDVI data are translated to NPP using MODIS (moderate-resolution imaging spectroradiometer) NPP data (Running and others 2004) for the overlapping period 2000-2003; this translation is approximate. From the year 2000, NPP has been calculated from MODIS measurements of the fraction of photosyntheticaly-active radiation absorbed by vegetation (which do not saturate at high leaf areas) at 1km resolution; this is the preferred indicator for the future.

The final caveat is that NDVI cannot be other than a proxy; it does not tell us anything about the kind of degradation or improvement - what is happening in, say, south China is different from what is happening in the Pampas, both in terms of the driving changes in land use and the symptoms of land degradation. We are using this indicator simply to identify *hot spots* of land degradation, and their counterpoint, *bright spots* of land improvement: land degradation is identified by a declining trend in climate-adjusted NDVI and land improvement by a rising trend. The patterns of land degradation and improvement, so identified, are further explored by comparisons with land cover, soil and terrain, and socio-economic data. In the parent LADA program, areas identified in this screening will be validated and characterized in the field by national teams.

2 Data and methods

2.1 Data

GIMMS (Global Inventory Modeling and Mapping Studies) radiometer (AVHRR) data are collected by National Oceanic and Atmospheric Administration satellites. These data are corrected for calibration, variations in solar and view zenith angle, El Chichon and Mt Pinatubo stratospheric aerosols, and other effects not related to vegetation change, and generalized to 8km grids for 15-day periods. Global data are currently available for the period July 1981-December 2003 (Tucker and others 2004).

NDVI-NPP correlation: To provide a measure that is amenable to economic analysis, the GIMMS NDVI time series has been translated to NPP using MODIS data (Justice and others 2002, Running and others 2004)[1] for the overlapping period 2000-2003. NPP was estimated by correlation with MODIS 8-day NPP values for the overlapping years of the GIMMS and MODIS datasets (2000-2003), re-sampling the annual mean MODIS NPP at 1km resolution to 8km resolution using nearest-neighbour assignment. The empirical relationship is:

$$NPP_{MOD17}\ [\text{kgC ha}^{-1}\ \text{year}^{-1}] = 1106.37 * \text{sum NDVI} - 564.55 \qquad [1]$$

(r = 0.83, n = 3 128 207)

Where NPP_{MOD17} is annual mean NPP derived from MODIS MOD17 Collection 4 data, and sum NDVI is the four-year (2000-2003) mean annual sum NDVI derived from GIMMS. Uncertainty is for slope ± 3.818, and for intercept ± 16.364.

VASClimO 1.1 comprises the most complete monthly precipitation data for 1951-2000, compiled on the basis of long, quality-controlled station records, gridded at resolution of 0.5°, from 9 343 stations (Beck and others 2005). Monthly rainfall values since January 1981 were used for this analysis.

CRU TS 2.1 comprises monthly values of various station-observed meteorological data from the beginning of the 20th century, gridded at 0.5^{o} resolution (Mitchell and Jones 2005). Monthly temperature values since January 1981 were used for this analysis.

Rain-use efficiency (RUE), represented by the ratio of annual sum NDVI and annual rainfall, was calculated from the VASClimO rainfall data.

---

[1] MOD17A3 is a dataset of terrestrial gross and net primary productivity computed at 1-km resolution and an 8-day interval. Though far from perfect (Plummer 2006), MODIS gross and net primary productivity are related to observed atmospheric CO_2 and the inter-annual variability associated with the ENSO phenomenon, indicating that MODIS NPP data are reliable at the regional scale (Zhao and others 2005, 2006), and the dataset has been validated in various landscapes (Fensholt and others 2004, 2006, Gebremichael and Barros 2006, Turner and others 2003, 2006).

Energy-use efficiency (EUE), represented by the ratio of annual sum NDVI to annual accumulated temperature (day degrees above $0^{o}C$), was calculated from CRU 2.1 monthly data.

***Trends analysis*:** trends of NDVI and NDVI derivatives were determined by linear regression; the absolute change (Δ) is the slope of the regression. The data were tested for temporal and spatial independence following Livezy and Chen (1983): when the absolute values of the autocorrelation coefficients of lag-1 to lag-3, calculated for a time series consisting of *n* observations, are not larger than the typical critical value, i.e. $1.96/\sqrt{n}$ corresponding to 5 per cent significance level, the observations in this time series can be accepted as being independent from each other. The T- test was used to arrange the slope values in classes showing strong or weak positive or negative trends:

$$T = b / se(b)$$

Where *b* is the estimated slope of the regression line between the observation values and time and *se(b)* represents the standard error of *b.*

The class boundaries were defined for 99, 95 and 90 per cent confidence levels.

RESTREND: following the general procedure of Wessels and others (2007), correlations were calculated for each pixel between annual sum NDVI and annual rainfall (for the southern hemisphere beginning October 1 through the following September, and for the northern hemisphere the calendar year). The regression equation enables prediction of sum NDVI according to rainfall. Residuals of sum NDVI (i.e. differences between the observed and predicted sum NDVI) for each pixel were calculated, and the trend of these residuals was analysed by linear regression.

Aridity index was calculated as *P/PET* where *P* is annual precipitation in mm and $PET = P/\sqrt{(0.9+(P/L)^2)}$ where $L = 300 + 25T + 0.05T^3$ and *T* is mean annual temperature (Jones 1997). Precipitation was taken from the VASClimO dataset, mean annual temperature from the CRU dataset.

Soil and terrain: The global Soil and Terrain database (SOTER) comprises harmonized spatial and soil-attribute data for terrain mapping units defined using the 90m-resolution SRTM digital elevation model (van Engelen and Wen 1995). For this study, a global landform database and dataset of key soil attributes for the LADA partner countries has been prepared at scale 1:1 million-scale (ISRIC 2008a,b).

Land cover: LC 2000 global land cover data (JRC 2003) have been generalised for preliminary comparison with NPP trends.

Population, urban areas and poverty indices: The CIESIN Global Rural-Urban Mapping Project provides data for population and urban extent, gridded at 30 arc-second resolution (CIESIN 2004). Sub-national rates of infant mortality and child underweight status and the gridded population for 2005 at 2.5 arc-minutes resolution (CIESIN 2007) were compared with indices of land degradation.

Comparisons between land degradation and other indices: Maps of the climate-adjusted NDVI index were overlaid on the other global maps. Corresponding comparative values were calculated, and correlation calculated for all pixels.

2.2 Analysis

GLADA employs a sequence of remotely sensed datasets and supplementary station-observed climatic data to identify areas of land degradation and improvement:

1. Simple NDVI indicators (NDVI minimum, maximum, maximum-minimum, mean, sum, standard deviation and coefficient of variation) are computed for the calendar year for the northern hemisphere, and for October to the following September for the southern hemisphere, encompassing a complete growing season. Each of these indicators has biological meaning (Appendix 3).
2. The annual sum NDVI, the aggregate of greenness, is used as the standard surrogate for annual biomass productivity. NDVI is translated to net primary productivity by correlation with MODIS data; trends are calculated by linear regression.
3. To distinguish between declining productivity caused by land degradation, and declining productivity due to other factors, it is necessary to eliminate false alarms. Rainfall variability and irrigation have been accounted for by:
    a. Identifying pixels where there is a positive relationship between productivity and rainfall;
    b. For those pixels, RUE has been considered: where productivity declined but RUE increased, we attribute the decline of productivity to declining rainfall; those areas are masked (urban areas are also masked);
    c. NDVI trends have been calculated for the remaining areas – i.e. pixels where there is a negative relationship between NDVI an rainfall and, also, pixels with a positive relationship but declining RUE; this is called RUE-adjusted NDVI;
    d. Land degradation is indicated by a negative trend of RUE-adjusted NDVI and is quantified as RUE-adjusted NPP;
4. As an additional indicator, the residual trend of sum NDVI (RESTREND) is calculated for all pixels.
5. Energy-use efficiency (EUE) is also considered to take account of the significant lengthening and warming of the growing season at high latitudes. EUE is calculated for all pixels but, in practice, scarcely affects the estimation of land degradation. Land improvement is indicated by a positive trend in both RUE-adjusted NPP and EUE, and is quantified as climate-adjusted NPP.

6. The indices of land degradation and improvement are compared with land cover; soil and terrain; rural population density; and indices of aridity and poverty.

Algorithms have been devised to undertake these screening analyses automatically. Details of the analytical methods are given as Appendix 2.

At the next stage of analysis, areas of land degradation and improvement identified on the basis of NDVI indicators will be characterised manually, using 30m-resolution Landsat data, to identify the probable kinds of land degradation.

At the same time, the continuous field of the index of land degradation derived from NDVI and climatic data will enable a statistical examination of other data for which continuous spatial coverage is not available - for instance spot measurements of soil attributes, and other social and economic data that may reflect the drivers of land degradation, provided that these other data are geo-located.

Finally, field examination of the identified areas of degradation and improvement will be undertaken by national teams within the wider LADA program.

3 Results

3.1 Greenness trends

Globally, greenness increased by 3.8 per cent (P < 0.05) for the period 1981-2003 but there are significant variations at the continental scale (Figure 1) and at country and regional scales (Bai and Dent 2007 a-f). The increase was 3 per cent in Africa and North America, 4.4 per cent in Latin America, 4.5 per cent in Australia, 5.4 per cent in Europe, and 6 per cent in Asia. Regional patterns commonly track the ENSO cycle - with losses during El Niño events and gains during La Nina events. Figure 2 depicts global change in NDVI, scaled in terms of NPP, over the period 1981-2003; ice and extreme desert with NPP less than 1gC m^{-2} are designated as *no change*

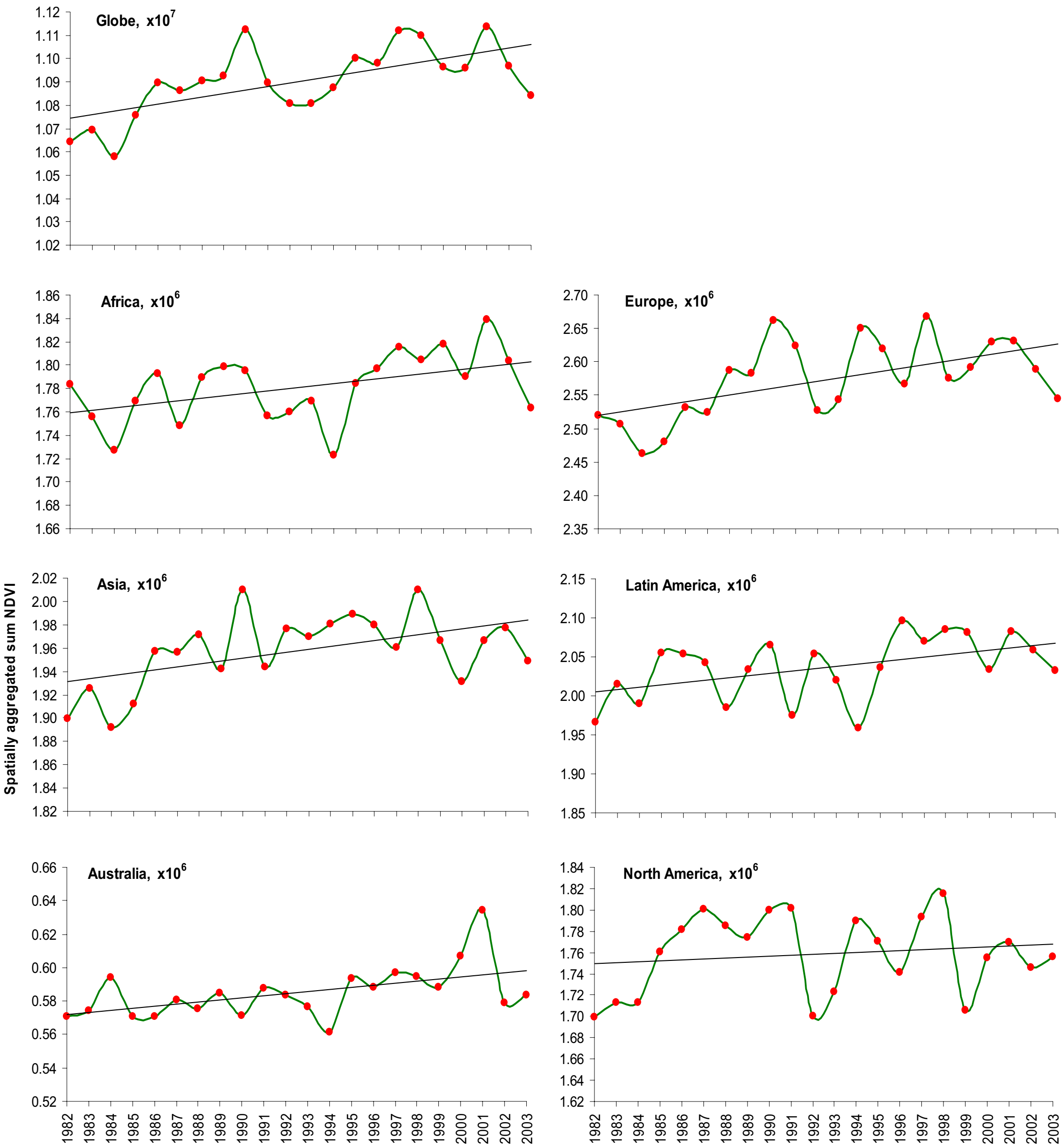

Figure 1. Spatially aggregated annual sum NDVI 1981-2003, *p*<0.01

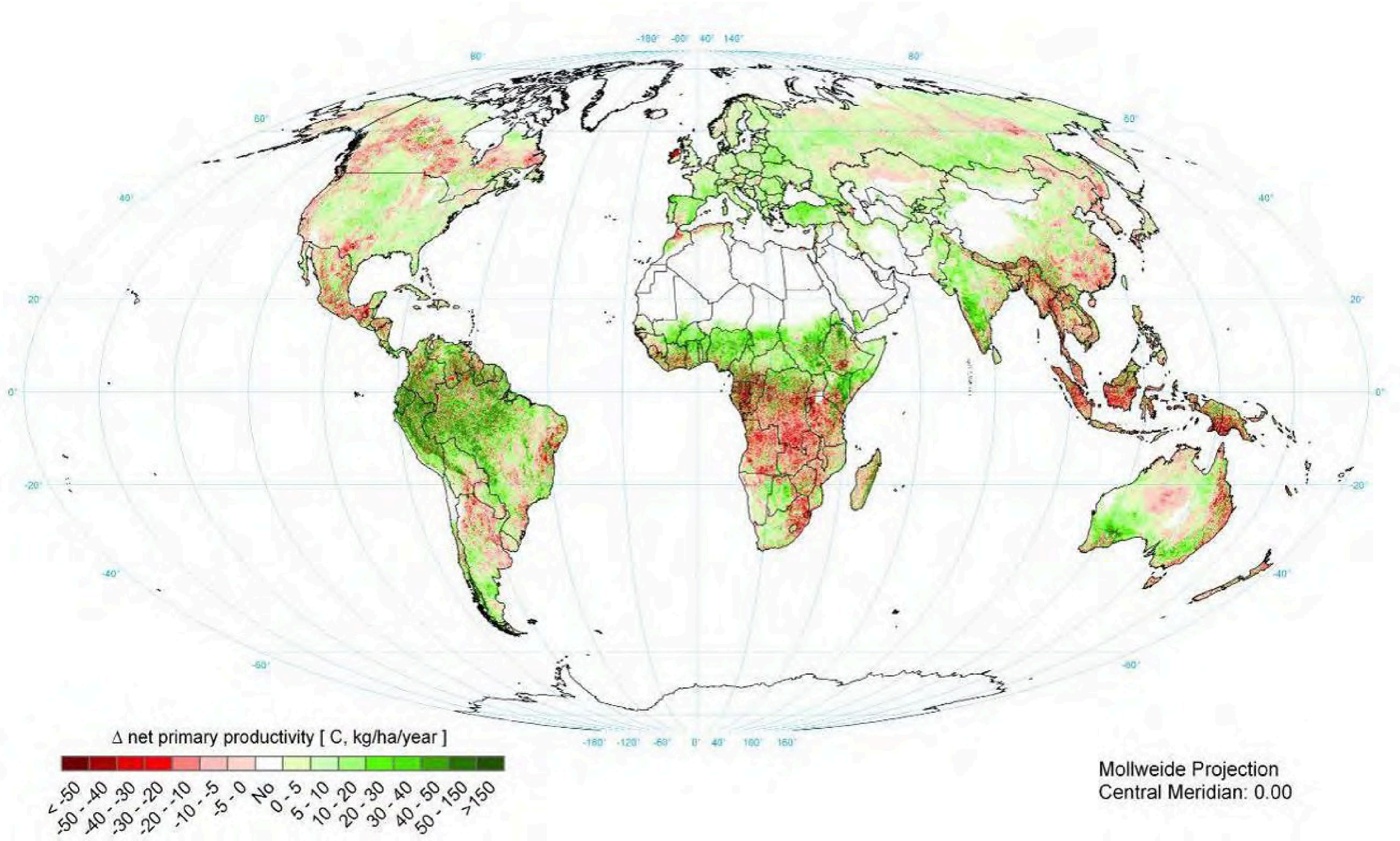

Figure 2. Global change in net primary productivity, 1981-2003

3.2 Climate-adjusted greenness

Two approaches are explored to allow for rainfall variability: calculation of rain-use efficiency and calculation of residual trends of observed NDVI from NDVI modelled from rainfall (RESTREND). In addition, energy-use efficiency is calculated from global temperature data.

3.2.1 Rain-use efficiency

Rain-use efficiency (RUE) is production per unit of rainfall. It may fluctuate dramatically in the short term; often there is a sharp decline in RUE when rainfall increases and we assume that the vegetation, whether cultivated or semi-natural, cannot make immediate use of the additional rain. But where rainfall is the main limiting factor on biomass productivity, we judge that the long-term trend of RUE is a good indicator of land degradation or improvement (Houérou 1984, Houérou and others 1988, Snyman 1998, Illius and O'Connor 1999, O'Connor and others 2001). Furthermore, pixel-by-pixel analysis of the rainfall–biomass production relationship accommodates the effects of local variations in slope, soil and vegetation (Justice and others 1991).

In North China and Kenya, Bai and others (2005, 2006) demonstrated that values for RUE calculated from NDVI, which are easy to obtain, were comparable with those calculated from field measurements of NPP, which are not easy to obtain. Globally, RUE was calculated as the ratio between annual sum NDVI and station-observed annual rainfall. Figure 3 maps global trends of RUE over the period 1981-2003.

Figure 4 depicts relationship between sum NDVI with rainfall. Drylands mostly show a positive relationship between RUE and rainfall; humid and cold regions, irrigated areas and some wetlands mostly show a negative relationship but there are some exceptions that may be related to land use change and/or land degradation.

For those pixels where there is a positive relationship, RUE was considered: where productivity declined but RUE increased, we attribute the decline in productivity to declining rainfall and those areas were masked. NDVI trends were calculated for the remaining areas – that is, pixels where there is a negative relationship between NDVI and rainfall (taken to be areas of rainfall surplus compared with transpiration needs, or irrigated, or areas depending on groundwater) and, also, pixels with a positive relationship *but declining RUE*.

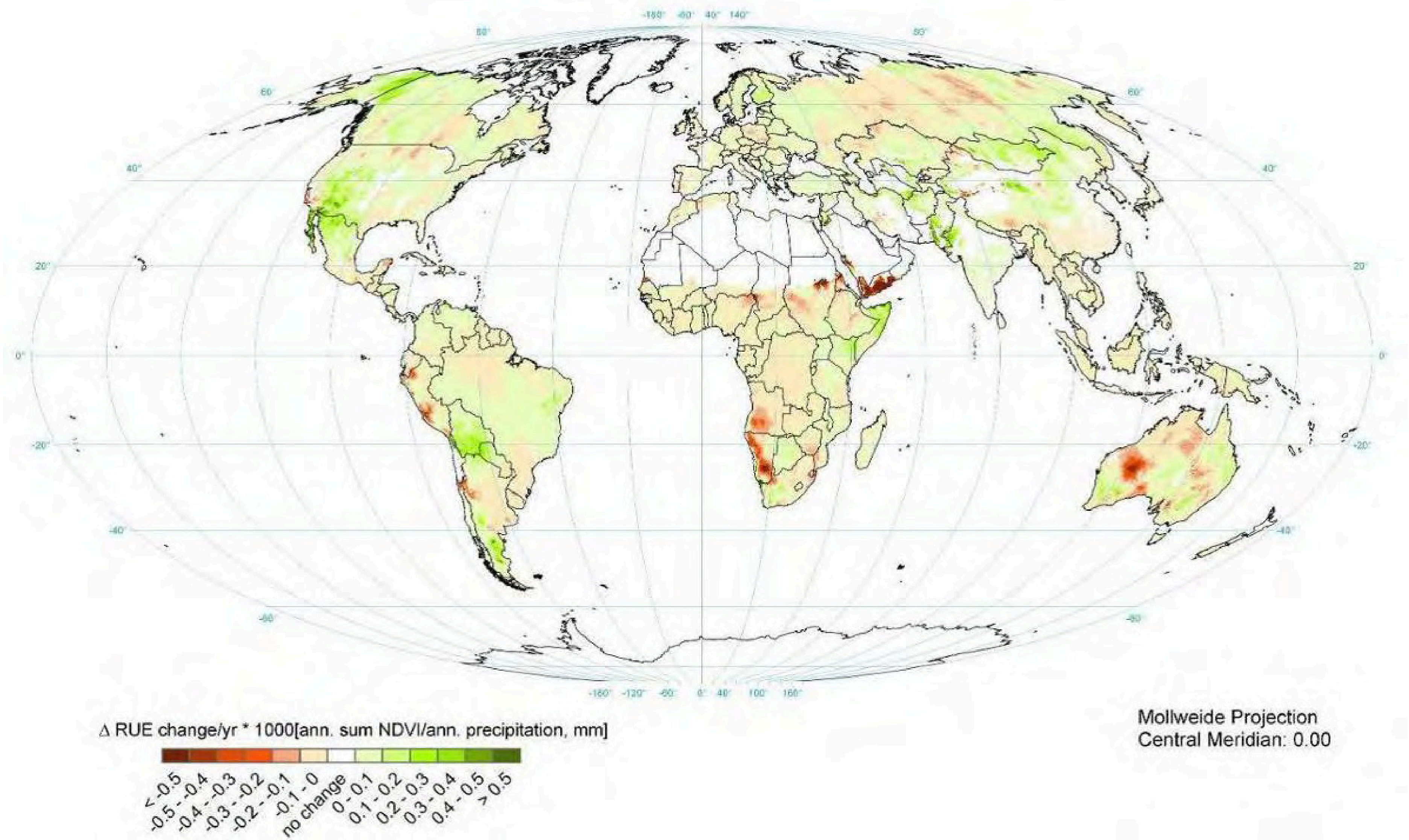

Figure 3. Global change in rain-use efficiency, 1981-2002

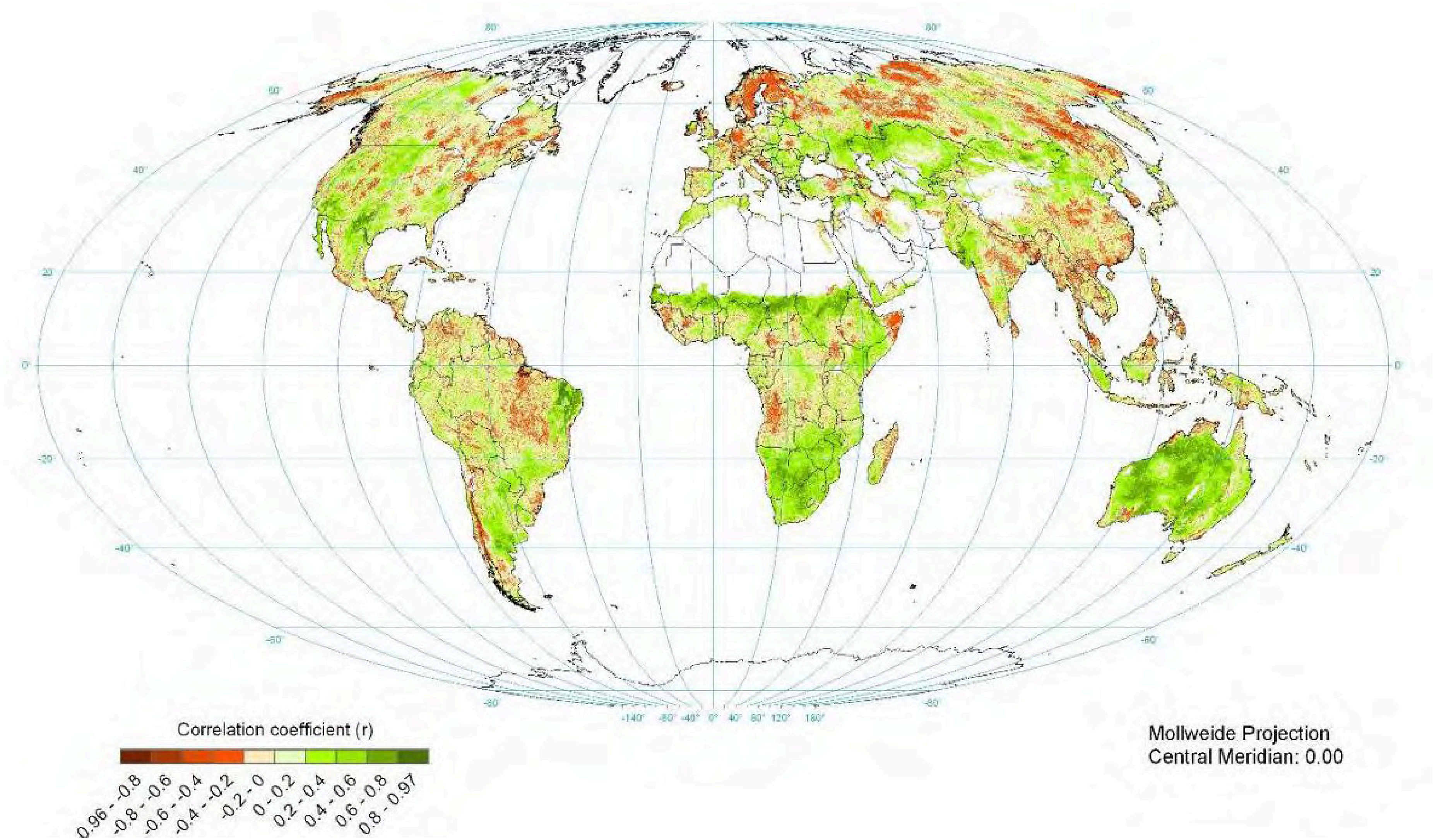

Figure 4. Correlation between annual sum NDVI and annual rainfall, 1981-2003

Figure 5 shows these areas as RUE-adjusted NDVI. As a first cut, we may equate declining RUE-adjusted NDVI with land degradation; these results have been validated by field observation in North China (Bai and others 2005) and independently by Chen & Rao (2008); Kenya (Bai & Dent 2006); and Bangladesh (Bai 2006).

Figure 6 shows the confidence levels of these RUE-adjusted negative trends in NDVI. Two per cent of the land area exhibits a negative trend at the 99% confidence level, 5 per cent at 95% confidence and 7.5 % at the 90% confidence level. The smallness of these areas may be explained by the coarse (8km) resolution of the GIMMS data. We see through a glass darkly; an area of land degradation much smaller than 8km across must be severe indeed to be seen through the signal from a much larger surrounding area.

3.2.2 RESTREND

Globally, there is a significant correlation between NDVI and rainfall (Figure 4). RUE also fluctuates along with fluctuations of rainfall. To get around correlations between RUE and rainfall, Wessels and others (2007) suggest the alternative use of Residual Trends to distinguish land degradation from the effects of rainfall variability. Following their general procedure, we correlated annual sum NDVI and annual rainfall for each pixel; the resulting regression equation represents the statistical association between observed sum NDVI and rainfall and allows for prediction of sum NDVI based on the rainfall.

Residuals of sum NDVI (differences between the observed and predicted sum NDVI) were calculated for each pixel and residual trend (RESTREND) was analysed by linear regression (Figure 7); its significance was assessed by the T-test (Figure 8).

RESTREND points in the same direction as RUE: negative values may indicate human-induced land degradation and positive values improvement.

3.2.3 Energy-use efficiency

Energy use efficiency (EUE) is calculated as the ratio of annual sum NDVI to accumulated temperature (day-degrees Celsius above zero). Figure 9 shows its trend over the period 1981-2002. The global increase in temperatures, especially at high latitudes, has been accompanied by a marked increase in NDVI (Figure 2) but not, in general, in the EUE of either natural vegetation or farmed land.

Combination of the negative EUE indicator with negative RUE-adjusted NDVI makes virtually no difference to the delineation of hotspots of land degradation. However, addition of the EUE indicator does make a big difference to the assessment of land improvement: Figure 10 maps the areas that exhibit *both* a positive trend in RUE-adjusted NDVI and positive EUE as Climate-adjusted NDVI; Figure 11 depicts the confidence levels.

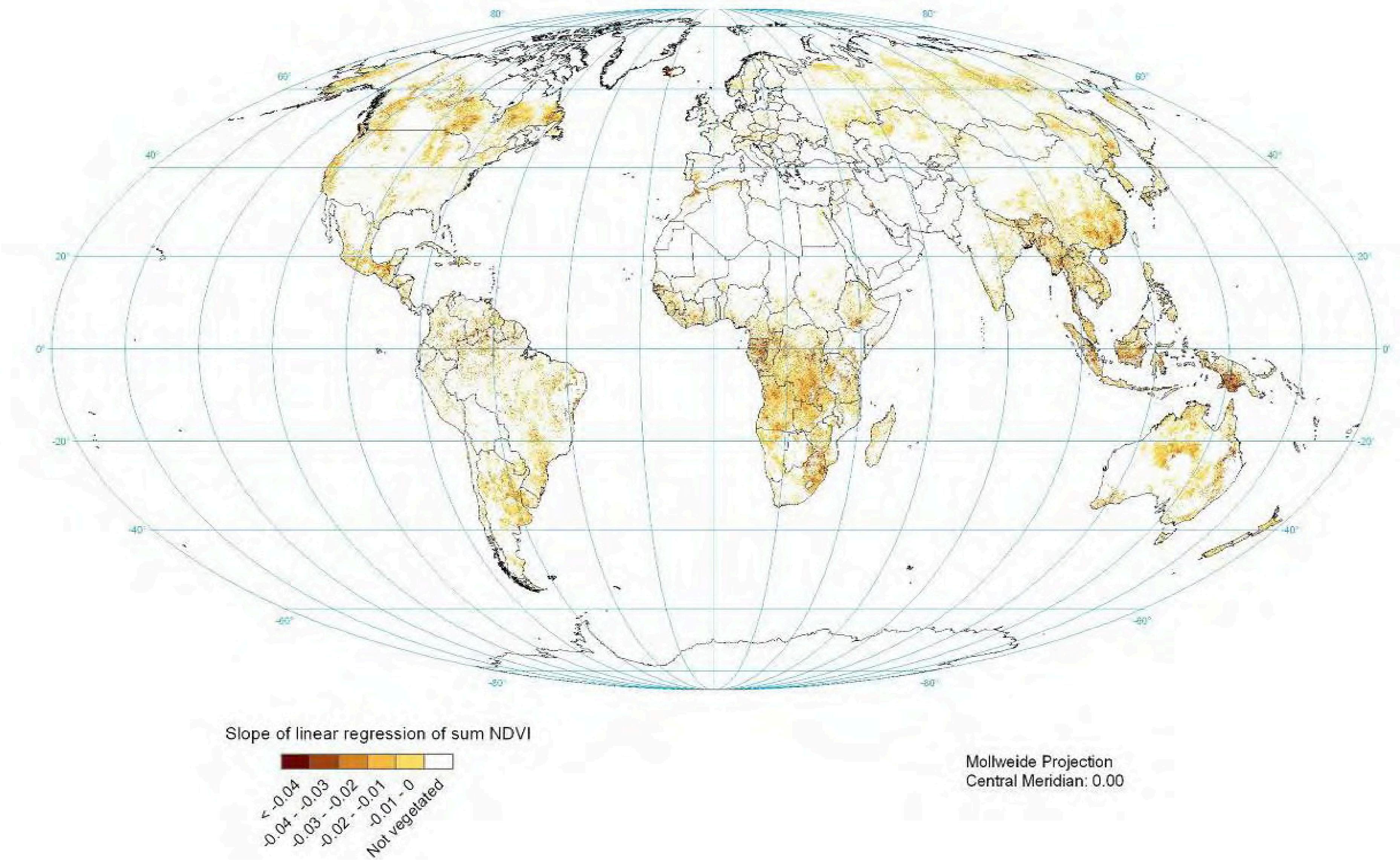

Figure 5. **Global negative trend in RUE-adjusted NDVI, 1981-2003**

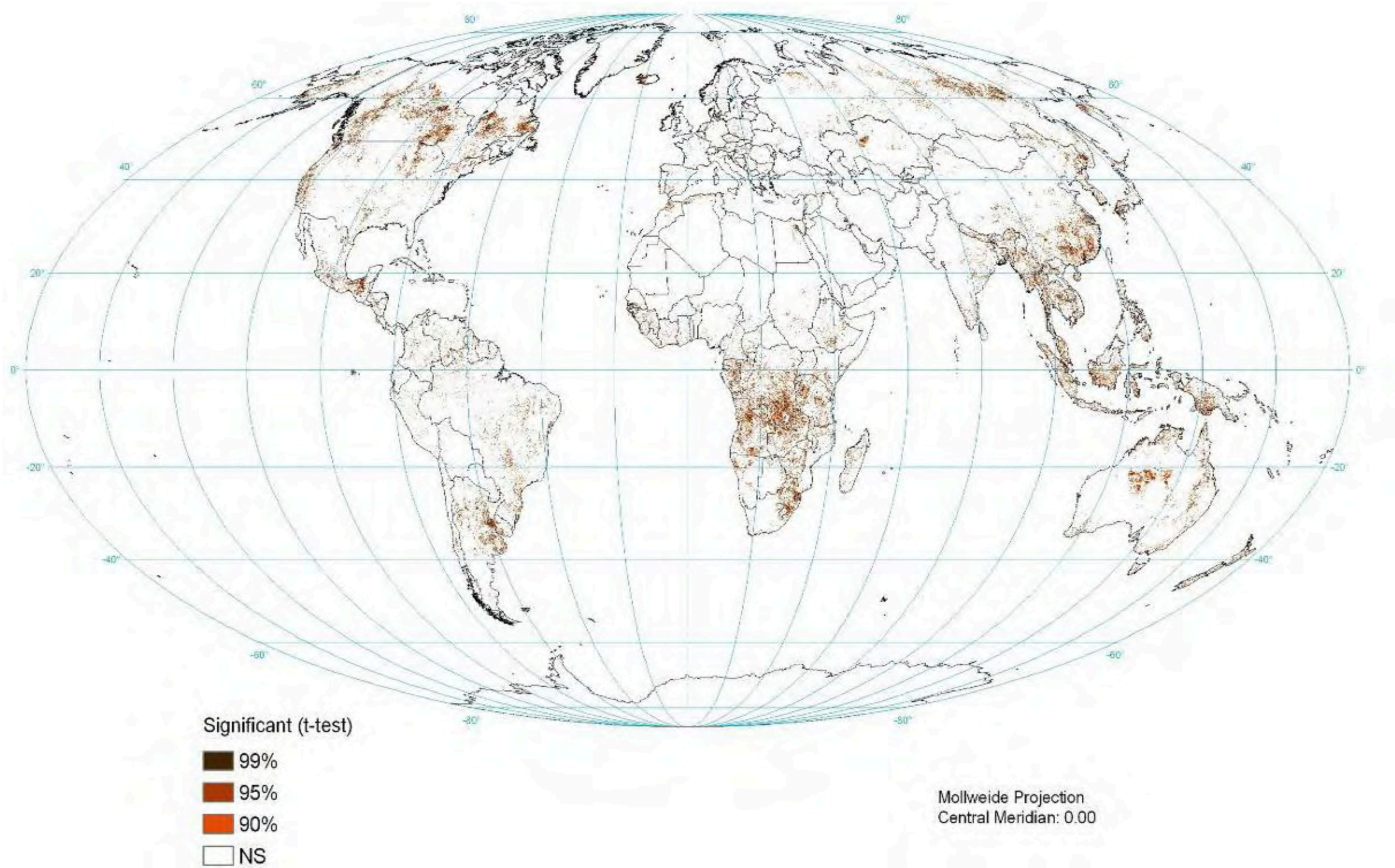

Figure 6. Confidence levels of RUE-adjusted sum NDVI, 1981-2003

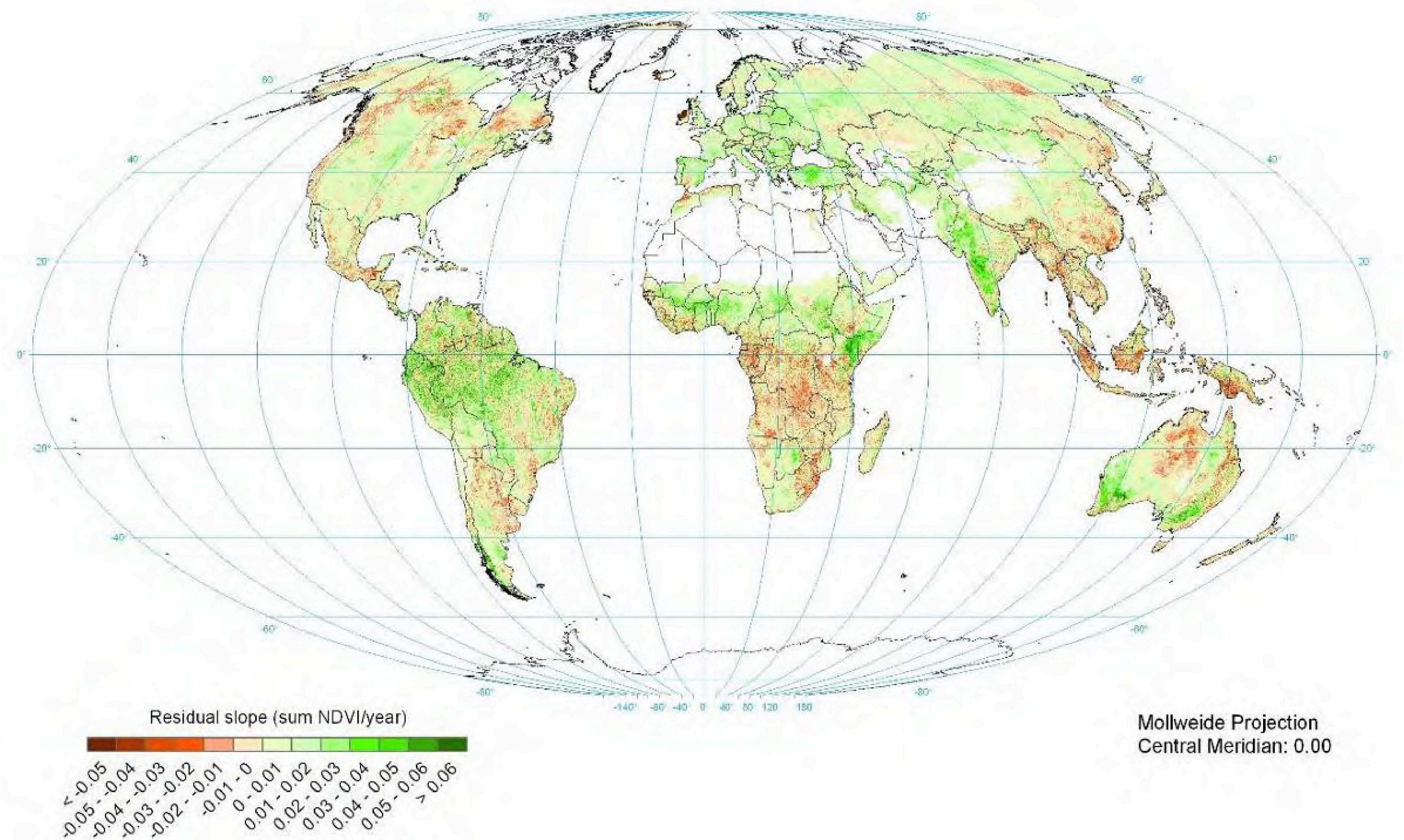

Figure 7. Residual trends of sum NDVI (RESTREND), 1981-2003

Figure 8. Confidence levels of RESTREND, 1981-2003

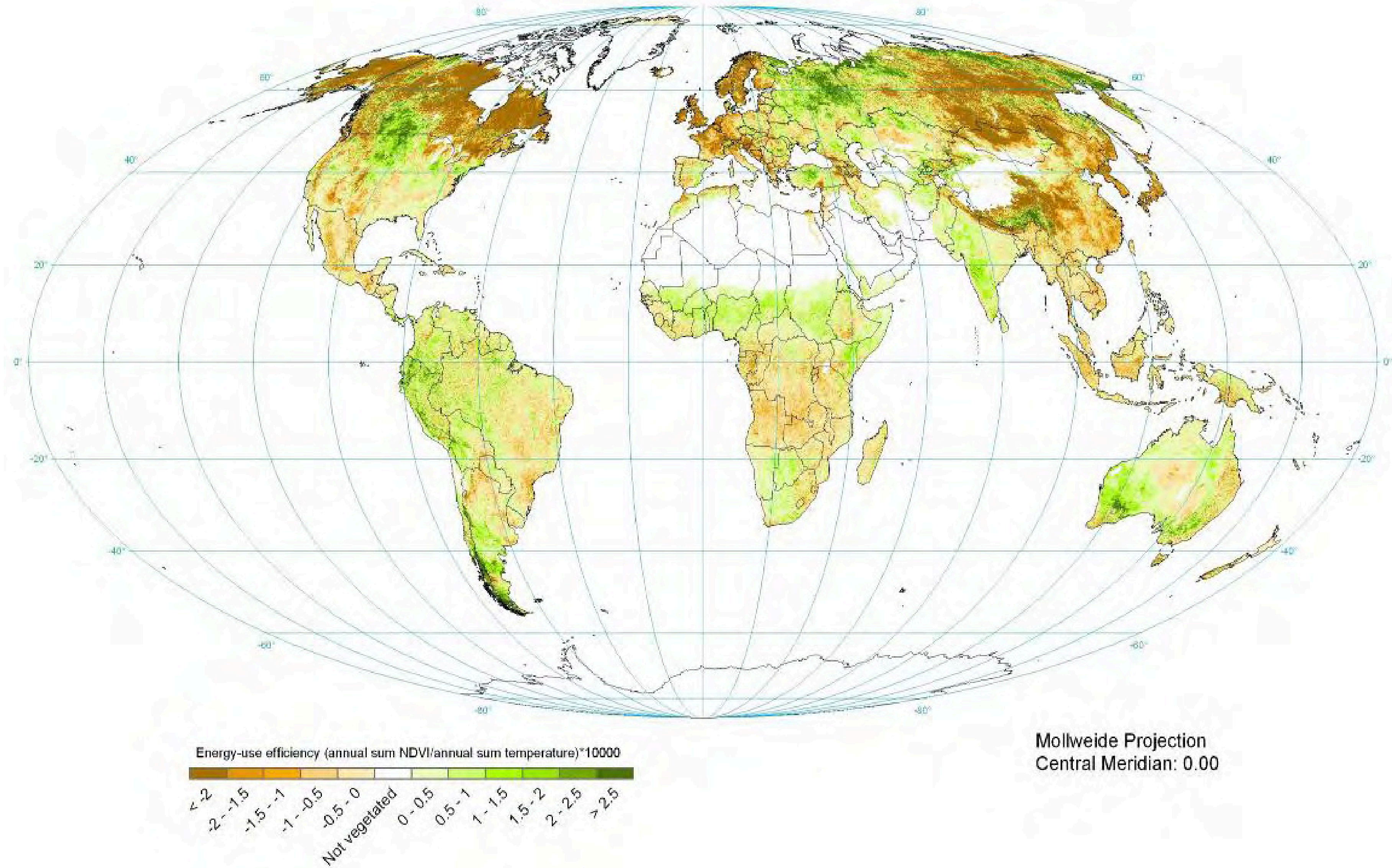

Figure 9. Global change in energy-use efficiency, 1981-2002

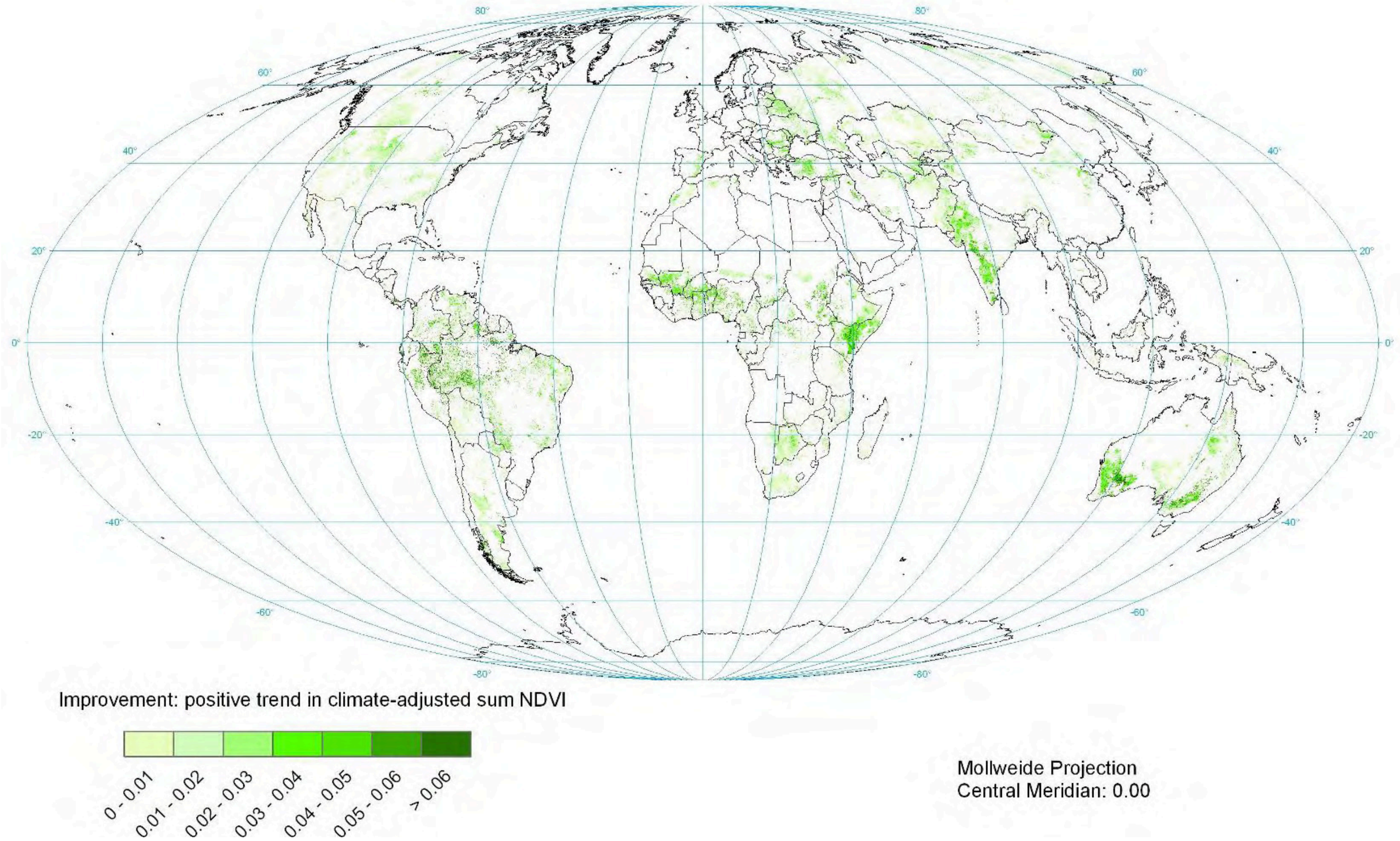

Figure 10. **Global trend of positive climate-adjusted NDVI, 1981-2003**

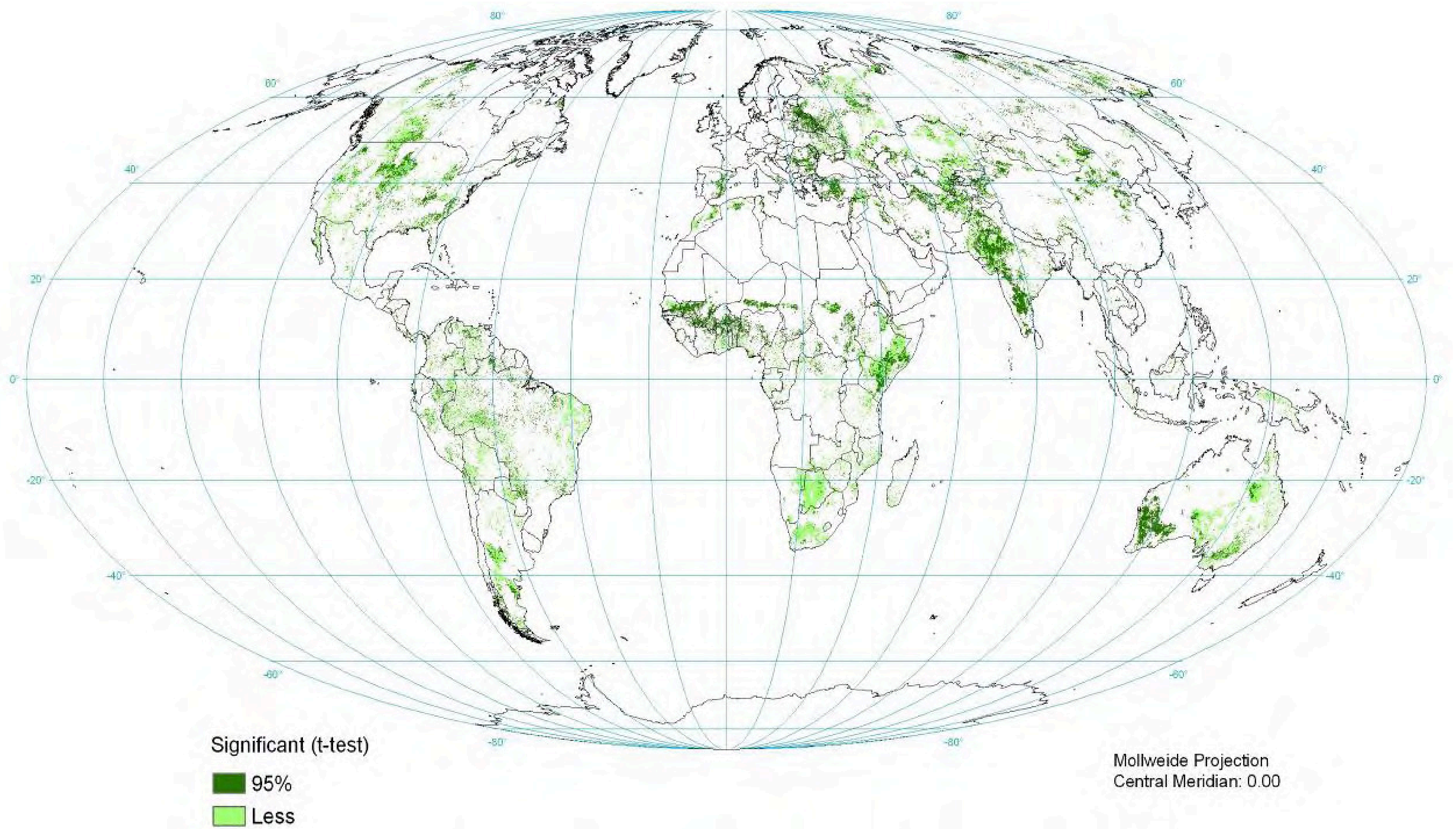

Figure 11. Confidence levels of positive climate-adjusted NDVI, 1981-2003

4 Land degradation and improvement

4.1 Land degradation

Land degradation means a loss of NPP but a decrease in NPP is not necessarily land degradation. False alarms have to be eliminated to distinguish between declining productivity caused by land degradation and declining productivity due to other factors.

Rainfall variability has been accounted for using RUE-adjusted NDVI (Figure 5) and, also, by RESTREND (Figure 7). Overall, RESTREND patterns are remarkably close to sum NDVI (Figure 2) but the amplitude of the range is less. Comparison of the results of RESTREND and RUE-adjusted NDVI shows little difference between them: globally, 96.2% of the identified degrading land by negative RUE-adjusted NDVI also show negative RESTREND; 99.9% of the identified improving land presents positive RESTREND as well. We conclude that the identification of hot spots and bright spots is biologically meaningful. However, we are unable to make allowance for changes in land use and management at the global level for lack of consistent time series data; this will be addressed in following reports for individual hotspots and bright spots.

The results are very different from the previous global assessment of land degradation (GLASOD) and challenge conventional wisdom. To address the questions posed at the outset, comparisons were made with global data for land cover, aridity, population density, infant mortality rates and proportion of underweight children under the age of five. The following discussion relates mainly to RUE-adjusted NDVI and its translation to NPP, which we may take as a proxy indicator of land degradation.

4.1.1 Which regions are hardest hit?

Areas severely affected (Table 1) include:

- Africa south of the Equator (13 per cent of global degrading area and 18 per cent of lost global NPP);
- Indo-China, Myanmar, Malaysia and Indonesia (6 per cent of the degrading area and 14 per cent of lost NPP;
- S China (5 per cent of the degrading area and 5 per cent of lost NPP);
- N-central Australia and parts of the western slopes of the Great Dividing Range (5 per cent of the degrading area and 4 per cent of lost NPP);
- The Pampas (3.5 per cent of the degrading area and 3 per cent of lost NPP);
- Swaths of the high-latitude forest belt in North America and Siberia.

The usual suspects - drylands around the Mediterranean, Middle East, South and Central Asia - are represented by only relatively small areas of degradation in southern Spain, the Maghreb, Nile delta, Iraqi marshes, and the Turgay steppe. The differences from the previous assessment arise because GLASOD compounded current land degradation with the legacy of centuries past. These are two different things; both are important; but most areas of historical land degradation have become stable landscapes – with a stubbornly low level of productivity. The present assessment deals only with 1981-2003 and we have no comparable data for earlier periods.

Table 1 presents country-by-country data for RUE-adjusted NDVI and NPP (countries with no degradation are not listed). The area data refer to pixels showing any declining trend - irrespective of degrees of confidence; by and large, the areas identified as high confidence are also those showing the most extreme trends - so intensity of degradation may be ranked more meaningfully according to total NPP loss than by gross degrading area.

Table 1. Statistics of degrading areas 1981-2003, by country*

Country	Degrading area (km^2)	% Territory	% global degrading area	Total NPP Loss (tonne C/23yr)	% total population	Affected people
Afghanistan	7658	1.17	0.025	62859	2.56	671770
Albania	2334	8.12	0.009	47250	4.29	137861
Algeria	63475	2.67	0.196	1977970	22.45	7168600
Andorra	281	60.00	0.001	2604	20.53	20865
Angola	828029	66.42	2.370	37602597	60.74	9263348
Argentina	902438	32.62	3.130	23556380	36.95	14455278
Armenia	743	2.49	0.003	13887	1.99	75632
Australia	1994268	25.94	6.182	46905279	11.31	2187493
Austria	28291	33.74	0.117	1835	21.51	1730745
Azerbaijan	2633	3.04	0.009	1230833	2.98	238076
Bahamas, The	4130	29.63	0.009	195146	32.01	19029
Bangladesh	68422	47.52	0.199	2851384	49.12	72728775
Belgium	5404	17.71	0.024	69560	13.48	1396093
Belize	3026	13.18	0.008	65978	16.94	39513
Benin	14155	12.57	0.041	373747	12.84	932170
Bhutan	27011	57.47	0.073	1705766	54.99	1332662
Bolivia	60339	5.49	0.175	1656319	16.39	1518038
Bosnia and Herzegovina	7737	15.13	0.030	157646	16.77	704321
Botswana	97831	16.30	0.284	4111881	30.74	476893
Brazil	1881702	22.11	5.381	63346318	26.67	46595573
Brunei	2663	46.15	0.008	127918	85.02	264401
Bulgaria	9139	8.24	0.035	178003	11.72	881122
Burkina Faso	9255	3.38	0.026	123795	8.26	1101414
Burundi	13516	48.56	0.037	972686	52.09	3881071
Belarus	4053	1.95	0.019	82416	2.56	254841
Cambodia	77958	43.06	0.225	2524942	24.03	3583464
Cameroon	151605	31.89	0.417	9657120	26.30	4326977
Canada	1985085	19.90	11.575	93963813	17.69	5509584
Cape Verde	375	9.30	0.001	12087	24.76	72997
Central African Republic	126927	20.37	0.356	3701988	23.27	894315
Chad	52735	4.11	0.152	627041	10.82	995721
Chile	77230	10.20	0.265	1950752	10.42	1645825
China	2193697	22.86	7.627	58840237	34.71	457202031

Country	**Degrading area (km^2)**	**% Territory**	**% global degrading area**	**Total NPP Loss (tonne C/23yr)**	**% total population**	**Affected people**
Colombia	291295	25.58	0.818	17999691	36.02	16309420
Comoros	181	8	0.001	17516	21.50	135144
Congo	201614	58.95	0.569	20091044	54.93	1895981
Costa Rica	14691	28.75	0.042	529400	13.41	592632
Croatia	2822	4.99	0.011	28610	7.95	338952
Cuba	32430	29.25	0.095	755492	28.31	3050838
Cyprus	266	2.87	0.001	9143	0.74	5164
Czech Republic	11218	14.22	0.048	304243	13.24	1358728
Demark	91	0.21	0.001	290	0.24	10824
Djibouti	6107	27.76	0.017	19272	59.30	282700
Dominica	126	16.67	0.000	8976	7.57	4532
Dominican Republic	18507	37.98	0.054	560541	43.43	3843087
Ecuador	40136	14.15	0.101	2401058	16.13	2199904
Egypt	36514	3.65	0.112	16639	13.92	10100710
El Salvador	5585	26.54	0.016	234649	16.76	1139730
Equatorial Guinea	15376	54.81	0.037	1434524	45.39	171542
Eritrea	15573	12.84	0.045	33256	5.27	235381
Estonia	423	0.93	0.003	4083	0.75	9180
Ethiopia	296812	26.33	0.843	14276064	29.10	20650316
Falkland Islands (Islas Malvinas)	1635	13.43	0.009	50944	23.18	365
Finland	27779	8.24	0.178	327719	3.46	171458
France	46691	8.54	0.190	605160	10.48	6159286
French Guiana	24947	27.41	0.064	1033318	14.36	25745
Gabon	172865	64.58	0.471	23880	35.85	468972
Gambia, The	1396	12.35	0.004	26355	1.93	25821
Georgia	5647	8.10	0.021	141370	11.76	591918
Germany	32479	9.10	0.144	730980	6.97	5676882
Ghana	50365	21.11	0.143	2520819	20.95	4466773
Greece	6914	5.24	0.024	116915	6.76	662921
Guatemala	55884	51.32	0.163	2866596	30.46	3936416
Guinea	91415	37.18	0.262	2008342	46.51	4108349
Guinea-Bissau	18851	52.19	0.048	452425	43.43	536156
Guyana	93448	43.47	0.257	230119	26.49	198445
Haiti	11821	42.60	0.034	383261	34.56	2823765
Honduras	30145	26.89	0.084	1450818	23.38	1673952
Hungary	31398	33.75	0.128	765915	28.90	2810672
Iceland	34483	33.48	0.225	2693154	23.51	58021
India	592498	18.02	1.751	22484086	16.50	177437809
Indonesia	1028942	53.61	2.703	67679850	40.52	86656550
Iran	29190	1.77	0.095	282438	3.42	2572958
Iraq	28000	6.41	0.092	1030763	6.58	1718397
Ireland	6416	9.13	0.035	1363385	11.95	653134
Israel	3085	14.85	0.010	49570	30.07	2035012
Italy	28693	9.53	0.109	696409	7.80	4306062
Ivory Coast	117595	36.47	0.331	6221305	36.33	6252711
Jamaica	3372	30.68	0.010	106751	28.98	741313
Japan	130563	34.56	0.451	4268668	24.20	29666795
Jordan	13574	15.21	0.048	100582	19.13	1574810
Kazakhstan	487083	17.93	2.041	5308145	13.31	2131386

Country	Degrading area (km^2)	% Territory	% global degrading area	Total NPP Loss (tonne C/23yr)	% total population	Affected people
Kenya	104994	18.02	0.294	6612571	35.59	11803311
Korea, Peoples Republic of	60959	50.57	0.226	2206450	45.08	10124149
Korea, Republic of	54091	54.93	0.182	1570729	31.81	14364205
Kyrgyzstan	23189	11.68	0.087	282173	12.71	682075
Laos	133395	56.33	0.382	7232762	55.13	3304253
Latvia	4416	6.84	0.022	136363	9.49	213414
Lebanon	704	6.77	0.002	1894	3.37	123717
Lesotho	10344	34.08	0.033	485251	44.49	941131
Liberia	50500	45.34	0.123	2097992	38.12	1441085
Libya	12672	0.72	0.037	86083	6.92	402408
Lithuania	2664	4.09	0.016	55190	2.91	132351
Macedonia	1757	6.94	0.007	32910	1.42	30073
Madagascar	163843	27.91	0.492	6678189	21.56	3901784
Malawi	30869	26.05	0.089	1370895	19.89	2486085
Malaysia	175817	53.32	0.475	9257510	46.39	10401113
Mali	35637	2.87	0.106	357823	6.60	870031
Mauritania	6301	0.61	0.019	17918	2.18	67349
Mexico	487804	24.73	1.474	23871309	34.30	36234761
Moldova	1751	5.17	0.007	32362	3.17	133140
Mongolia	66559	4.25	0.271	623762	2.51	66138
Morocco	67399	15.09	0.201	2807952	35.71	11278600
Mozambique	226567	28.26	0.651	8398073	26.36	5155480
Myanmar (Burma)	358887	52.89	1.053	23625068	47.86	23608512
Namibia	288945	35.01	0.875	6388447	35.87	670983
Nepal	54704	38.85	0.182	2375267	48.93	13332932
Netherlands	7051	16.98	0.028	92199	17.25	2779551
New Caledonia	6902	36.21	0.020	1008271	31.44	48235
New Zealand	147014	54.72	0.545	6992963	30.97	1015925
Nicaragua	47223	36.47	0.134	2060424	29.28	1684227
Niger	22563	1.78	0.062	141699	6.61	844506
Nigeria	91443	9.90	0.256	3066735	13.33	17035650
Norway	57109	17.61	0.352	1212969	9.23	361786
Oman	419	0.20	0.002	3302	0.06	1848
Pakistan	20644	2.57	0.073	235711	3.58	5838072
Panama	8735	11.17	0.023	513509	7.78	232958
Papua New Guinea	205500	44.40	0.564	16275368	40.58	2019646
Paraguay	66704	16.40	0.200	1659008	66.97	4071629
Peru	197211	15.34	0.565	11414777	10.89	3001345
Philippines	132275	44.09	0.362	4100145	42.75	33064628
Poland	41514	13.28	0.188	890969	14.37	5505161
Portugal	11536	12.49	0.041	233458	4.58	440851
Puerto Rico	436	4.79	0.001	19231	2.91	111458
Reunion	175	6.98	0.001	6294	5.24	38724
Romania	16902	7.12	0.067	364407	4.47	980580
Russia	2802060	16.41	16.519	56663083	6.20	8588604
Rwanda	11404	43.30	0.031	1053147	39.11	3299059
Sao Tome and Principe	125	12.50	0.000	303560	21.82	28128
Saudi Arabia	8327	0.42	0.025	4335	2.00	471248

Country	Degrading area (km^2)	% Territory	% global degrading area	Total NPP Loss (tonne C/23yr)	% total population	Affected people
Senegal	34655	17.66	0.101	408832	20.49	2078643
Sierra Leone	35902	50.04	0.102	1507871	39.33	2103046
Singapore	243	37.50	0.001	5833	55.95	2017090
Slovakia	5066	10.37	0.021	110642	6.86	370606
Slovenia	2492	12.30	0.010	38132	17.99	396448
Solomon Islands	9065	31.86	0.030	628541	33.82	206290
Somalia	52520	8.24	0.149	1834048	14.77	1544921
South Africa	351555	28.82	1.124	23123364	38.14	17041101
Spain	63266	12.53	0.231	1712506	6.41	2417996
Sri Lanka	21057	32.09	0.060	634813	25.62	4788637
Sudan	166031	6.63	0.480	3627514	9.43	3280414
Suriname	50503	30.93	0.125	2102420	10.13	38529
Swaziland	16533	95.22	0.051	1226857	98.77	947510
Sweden	78964	17.55	0.475	1594303	10.37	841284
Switzerland	4982	12.07	0.020	106619	6.81	484619
Syria	11327	6.12	0.039	224233	6.71	1243265
Tajikistan	8412	5.88	0.030	104021	2.39	151676
Tanzania, United Republic of	386256	40.87	1.081	22603896	39.48	15300003
Thailand	309245	60.16	0.895	15990860	56.66	36991080
Togo	11064	19.48	0.032	2992723	12.79	654476
Trinidad and Tobago	675	13.16	0.002	113407	5.51	65120
Tunisia	12476	7.63	0.040	398423	15.47	1512817
Turkey	30851	3.95	0.111	453231	5.08	3571290
Turkmenistan	1273	0.26	0.005	8417	0.33	17554
Turks and Caicos Islands	92	21.43	0.001	15961	21.49	166
Uganda	41506	17.58	0.120	1513212	15.04	4112702
Ukraine	47414	7.85	0.200	1048460	5.25	2466172
United Kingdom	23506	9.60	0.103	262090	5.95	3324064
United States	1983886	20.60	7.935	39672698	10.79	31144568
Uruguay	87566	49.69	0.294	1874537	33.03	1058877
Uzbekistan	5974	1.34	0.022	123701	2.22	585887
Vanuatu	2210	14.97	0.005	4589	9.61	16965
Venezuela	207916	22.80	0.587	520023	8.28	2156456
Vietnam	134026	40.67	0.387	342632	35.27	28085074
Yemen	14422	2.73	0.032	7570	2.30	507751
Yugoslavia(Macedonia, Serbia, Montenegro)	10507	8.23	0.032	27197	6.37	678700
Zaire (Dem. Republic Congo)	1346914	57.43	3.760	3403930	53.49	32081359
Zambia	454630	60.41	1.312	19900481	50.07	5789865
Zimbabwe	180125	46.12	0.531	8861748	39.51	5424488
The World (land, excluding inland water body)	35058104	23.54	100.000	955221418	23.89	1537679148

*Countries or regions without degradation are not listed

The country ranking of severity of land degradation by proportion of the global degrading area is 1 Russia (16.5 per cent), 2 Canada (11.6), 3 USA (7.9), 4 China (7.6), 5 Australia (6.2); rank by loss of NPP (million tonneC) is 1 Canada (94), 2 Indonesia (68), 3 Brazil (63), 4 China (59), 5 Australia (50); rank by proportion of the country affected is 1 Swaziland (95 per cent), 2 Angola (66), 3 Gabon (64), 4 Thailand (60), 5 Zambia (60); and rank by rural population affected (millions) is 1 China (457), 2 India (177), 3 Indonesia (86), 4 Bangladesh (72), 5 Brazil (46). Table 2 shows the ranking of the LADA partner countries; China, Argentina and South Africa rank amongst the 20 most severely affected in terms of percentage area, loss of NPP and affected rural population. Each partner country is analysed individually in country reports (Bai and Dent 2007 a-f).

Table 2. Land degradation in LADA partner countries by global rank order

	% global area	NPP loss, million tonnes C	% country affected	affected rural population, million
China	4 (7.6)	4 (58.8)	(23)	1 (457)
Argentina	8 (3.1)	10 (23.6)	(33)	17 (14)
South Africa	15 (1.1)	11 (23.1)	(29)	14 (17)
Cuba	(0.09)	(0.8)	(29)	(3)
Senegal	(0.1)	(0.4)	(18)	(2)
Tunisia	(0.04)	(0.4)	(8)	(1.5)

4.1.2 Is land degradation a global issue?

Over the last 25 years, 24 per cent of the land area has been degrading (Table 1); this is on top of the legacy of thousands of years of mismanagement in some long-settled areas. GLASOD estimated that 15 per cent of the land was degraded (Appendix Table S1), and those areas are, by and large, not the same as the areas highlighted by the new analysis; land degradation is cumulative - this is the global issue.

Degrading areas directly affecting the livelihoods of 1.5 billion people. In terms of C fixation, degrading areas represent a loss of NPP of 9.56×10^8 tonneC relative to the 1981-2003 mean; that is 9.56×10^8 tonneC *not* removed from the atmosphere - equivalent to 20 per cent of the global CO_2 emissions for 1980. At the shadow price for carbon used by the British Treasury in February 2008 ($50/tonneC, Montbiot 2008) this amounts to $US 48 billion in terms of lost C fixation. But the cost of land degradation is at least an order of magnitude greater in terms of C *emissions* from loss of soil organic carbon: as much as one third of the human-induced increase in atmospheric CO_2 and 20 per cent of global carbon emissions over the period 1989-1998 is related to land use change (IPCC 2000, Houghton 2008).

4.1.3 Is land degradation mainly associated with farming?

Comparison of degrading areas with global land cover (JRC 2003, Table 2) reveals that 19 per cent of degrading land is cropland, 24 per cent is broadleaved forest, and 19 per cent needle-leaved forests. Cropland occupies only 12 per cent of the land area (and some of a further 4 per cent of mixed cover), so degradation is over-represented in cropland globally.

In Kenya over the period 1981-2003, NPP increased in woodland and grassland, but hardly at all in cropland; across 40 per cent of cropland it decreased - a critical situation in context of a doubling of human population over the same period (Bai and Dent 2006). In South Africa, NPP decreased overall; 29 per cent of the country suffered land degradation, including 41 per cent of all cropland (Bai & Dent 2007a); about 17 million people, 38 per cent of the South African population, depend on these degrading areas (Figure 12).

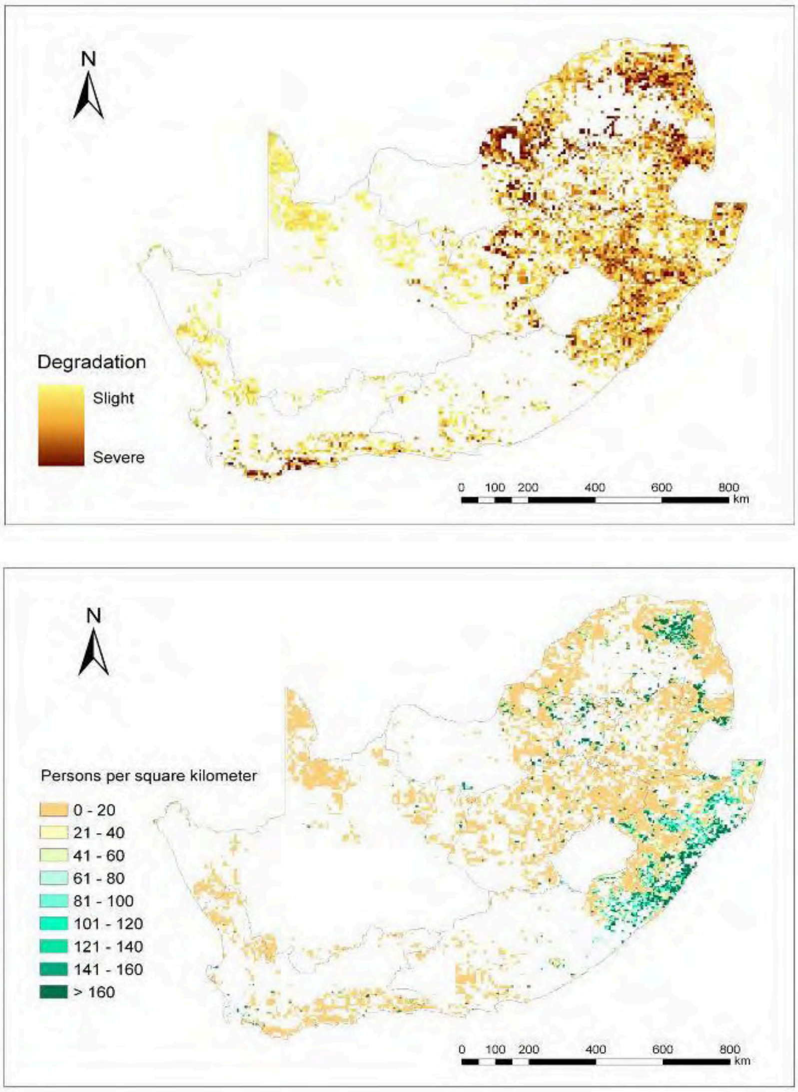

Figure 12. South Africa, land degradation and population affected, 1981-2003

Table 3. Global degrading and improving areas by land cover

Code	Land cover	Total pixels (TP)	Degrading pixels (DP)	DP/TP	DP/TDP*	Improving pixels (IP)	IP/TP	IP/TIP**
		(0.54'x0.54')	(0.54'x 0.54')	(%)	(%)	(0.54'x 0.54')	(%)	(%)
1	Tree Cover, broadleaved, evergreen	12875179	4222561	32.8	12.0	1985215	15.4	8.4
2	Tree Cover, broadleaved, deciduous, closed	8688097	2441119	28.1	6.9	877346	10.1	3.7
3	Tree Cover, broadleaved, deciduous, open	4099003	1616582	39.4	4.6	584110	14.3	2.5
4	Tree Cover, needle-leaved, evergreen	15080165	4633961	30.7	13.2	1020344	6.8	4.3
5	Tree Cover, needle-leaved, deciduous	8054159	2043323	25.4	5.8	427842	5.3	1.8
6	Tree Cover, mixed leaf type	5606446	993934	17.7	2.8	540412	9.6	2.3
7	Tree Cover, regularly flooded, fresh water	579763	228306	39.4	0.6	88405	15.2	0.4
8	Tree Cover, regularly flooded, saline water	115705	26157	22.6	0.1	17109	14.8	0.1
9	Mosaic: Tree Cover / Other natural vegetation	4269938	1097533	25.7	3.1	341516	8.0	1.4
10	Tree Cover, burnt	587270	225758	38.4	0.6	26659	4.5	0.1
11	Shrub Cover, closed-open, evergreen	3195387	1093184	34.2	3.1	226048	7.1	1.0
12	Shrub Cover, closed-open, deciduous	15605651	2953414	18.9	8.4	3263251	20.9	13.8
13	Herbaceous Cover, closed-open	17560702	2824775	16.1	8.0	3432708	19.5	14.5
14	Sparse herbaceous or sparse shrub cover	23573022	2567417	10.9	7.3	3115678	13.2	13.2
15	Regularly flooded shrub and/or herbaceous cover	3089962	689713	22.3	2.0	309398	10.0	1.3
16	Cultivated and managed areas	21692769	4522988	20.9	12.9	4306250	19.9	18.2
17	Mosaic: cropland/tree cover/other natural vegetation	4025653	1293550	32.1	3.7	559244	13.9	2.4
18	Mosaic: cropland/shrub and/or grass cover	3921904	692613	17.7	2.0	860554	21.9	3.6
19	Bare areas	24629888	931207	3.8	2.7	1641881	6.7	6.9
22	Artificial surfaces and associated areas	378999	35442	9.4	0.1	27944	7.4	0.1
23	No data	29056	120	0.4	0.0	50	0.2	0.0
Total		177658718	35133657	19.8	100.0	23651964	13.3	100.0

* TDP - Total degrading pixels; **TIP – Total improving pixels; water, snow and ice are excluded.

Land use and management change: may also generate false alarms. Conversion of forest or grassland to arable, pasture or even perennial crops will usually result in an immediate reduction in NPP (and NDVI) but may well be profitable and sustainable, depending on management. Lack of consistent time series data for land use and management precludes a generalised analysis of land use change but this can be undertaken manually for the potential *hot spots* of land degradation, e.g. Chen and Rao 2008.

4.1.4 Land degradation a dryland issue?

Drylands do not figure strongly in ongoing land degradation, apart from in Australia. Indeed, the recovery of the Sahel from the droughts of the 1980s is a notable feature (Figure 2 and Olsson and others 2005). Globally, there is little correlation (r = -0.12) between land degradation and Turc's aridity index; 78 per cent of degradation by area is in humid regions, 8 per cent in the dry sub-humid, 9 per cent in the semi-arid, and 5 per cent in arid and hyper-arid regions.

4.1.5 Is it related to population pressure?

Comparison of rural population density (CEISIN 2007) with land degradation shows no simple pattern. Globally, the correlation coefficient is -0.3; in general, the more people the less degradation. However, in some contexts, population pressure is positively related to land degradation; for South Africa (Figure 12, Figure 13), the correlation between land degradation and $\log_e$ population density is positive (r = 0.25) but the former apartheid homelands have more than their fair share of degrading land (Bai and Dent 2007a) so something more than simple rural population density is at work.

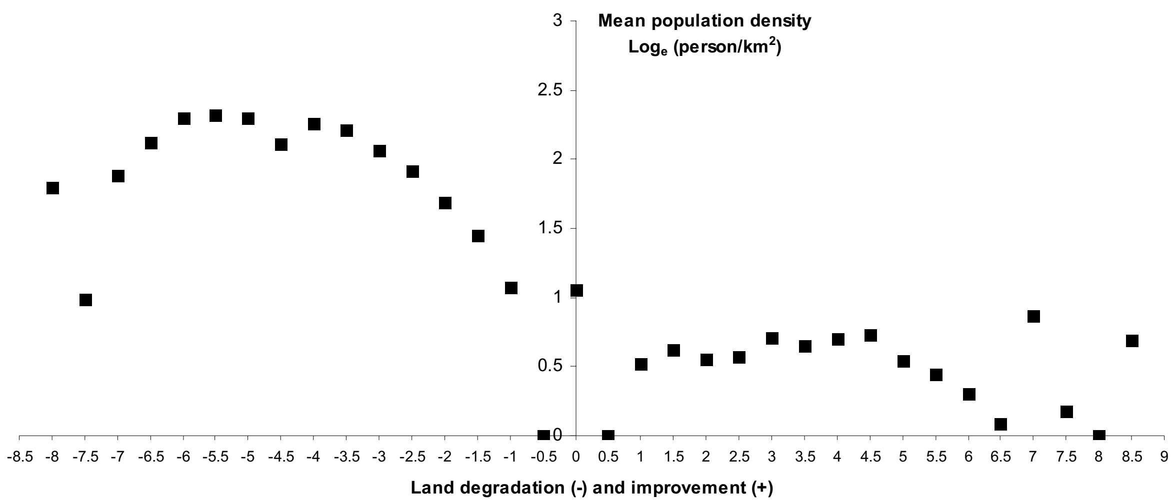

Figure 13. South Africa: relationship between population density and land degradation / improvement

4.1.6 Is land degradation related to poverty?

Taking infant mortality rate and the percentage of children under five who are underweight (CEISIN 2007) as proxies, there is some global relationship between land degradation and poverty: correlation coefficients are 0.20 for both infant mortality and for underweight children. However, a much more rigorous analysis is needed, especially to tease out the underlying biophysical and social and economic variables. This might be done using more specific geo-located data.

4.2 Land improvement

Land improvement is identified by: 1) a positive trend in NDVI-adjusted sum NDVI and 2) a positive trend in energy-use efficiency (Figure 10). These areas account for 15.7 per cent of the land area. Eighteen per cent is cropland (20 per cent of the total croplands), 23 per cent is forest and 43 per cent rangeland. Many gains in cropland are associated with irrigation but there are also swaths of improvement in rain-fed cropland and pastures in the Prairies and Great Plains of North America, and western India.

Some of the NDVI gains are a result of increasing tree cover, either through forest plantations, especially in Europe and North America (FAO 2006), and some significant land reclamation projects, for instance in North China. However, some of the positive trends represent woodland and bush encroachment into rangeland and farmland - which is not generally regarded as land improvement.

In spite of the attempt to eliminate false signals using RUE and RESTREND, the values for the Sahel probably show an element of recovery from the devastating drought of the early 1980s.

We may also attribute a general increase in greenness to the increasing trends of atmospheric CO_2 concentrations and nitrate deposition. Lower rainfall in the Amazon basin has been accompanied by decrease in growth-limiting cloudiness, but global data for net incoming radiation are not available to check this.

5 Future development

Some inherent limitations to the datasets used in this report have already been flagged: the 8-km resolution of the GIMMS data; saturation of the NDVI signal by dense vegetation leading to a lack of precision for forest mapping in particular; interference by cloud in perennially cloudy areas; and the scant rainfall observations in many parts of the world.

1. A new GIMMS dataset further corrected and updated to 2006, will be available soon. The VASClimO dataset is not yet updated to 2006; this is also expected later this year and will enable updating of the present analysis. More detailed analysis is possible for those areas that have higher resolution time series data, notably South Africa (Wessels and others 2004);
2. As an indicator of land degradation and improvement, f_{PAR} is preferred to NDVI – in its own right as a direct measurement of an important biophysical parameter, and to derive NPP through either the MODIS or JRC model. Data are available from year 2000 and, importantly, at 1km resolution rather than the 8km resolution of GIMMS. Looking forward, these data would be preferred for monitoring and early warning;
3. Rather than using sometimes-sparse station–observed data, rainfall modelled from earth-observation satellite data are now available at the same level of precision as f_{PAR}, data, e.g. TRMM (2008) and WaterWatch (2008). Again, this is preferred for the future but not applicable to the present analysis;
4. Cloud interference may be minimised by calculating trends for longer time steps, up to five years rather than an annual. This entails loss of precision.

The present analysis used only a fraction of the information available in the GIMMS data:

1. We have used simple linear regression of the 23-year GIMMS period to analyse the trends of NDVI and NDVI derivatives. It is possible to use power functions and separate, say successive 10-year periods;
2. There is valuable information in the seasonal shape of the NDVI curves that may be analysed, e.g. by harmonic analyses of NDVI time series (HANTS, de Wit 2004);
3. Critical information on timing of changes in land use and management can interpreted manually from time series for individual pixels but algorithm development is required for regional and global application;
4. Visualization can be greatly improved by three-dimensional overlays of the NDVI/NPP trend surfaces over topography and in combination with other data layers;
5. Comparison of the present situation with potential biological productivity without human-induced land use change – the Garden of Eden scenario – modelled from climatic, soils and topographic data using, e.g. the BIOME-BGC model (Thornton and others 2005), will enable separation of the last 25 years of land degradation from the historical legacy.

6 Conclusions

1. **Land degradation and improvement have been assessed by remotely sensed indicators of biomass productivity.** The indicators show clear regional trends over the period 1981-2003, both decreasing and increasing, which may be interpreted as land degradation or improvement, respectively.

2. **Biomass trends depend on several factors other than land degradation and improvement:**

   a. **We have taken account of rainfall variability in two ways: by screening NDVI trends for rain-use efficiency (RUE) in those areas where productivity is limited by rainfall, and by residual trends analysis.** RUE (net primary productivity per unit of rainfall), accounts for rainfall variability and, to some extent, local soil and land characteristics. We assume that, where NPP is limited by rainfall, a declining trend in RUE indicates land degradation where rainfall is not limiting; NDVI/NPP is the best indicator available. Taken together, the two indicators may provide a more robust assessment than either used alone. As well as RUE, we calculated residual trends of NDVI, which point in the same direction as RUE-adjusted NDVI;

   b. **Energy-use efficiency** (the ratio of NPP and accumulated temperature) proves to be more of an issue in defining improving areas than degrading areas;

   c. **Potentially significant factors for which there are no consistent global data include changes in land use and management** and net incoming radiation.

3. **All changes measured by climate-adjusted NDVI/NPP are not land degradation or improvement as usually understood***.* Change of land use from forest to cropland of lesser biological productivity, or an increase in grazing pressure, or a market adjustment to a less-intensive management will all decrease NDVI. However, these changes may or may not be accompanied by soil erosion, salinity, or other symptoms of land degradation of concern to soil scientists. Again, ambiguous data from the boreal forest belt may reflect periodic forest fires and recent mortality associated with outbreaks of pests, for instance the mountain pine beetle (Kurz and others 2008); these are part of the natural cycle but massive events falling towards the end of the 23-year measurement period affect the NDVI trend. This may not be land degradation - we should expect recovery - but if these events are themselves be related to climate change the system may not recover. In the same way, pastoralists will not consider bush encroachment as land improvement although it may increase biomass. These are all limitations of a proxy indicator.

4. **GLADA presents a different picture from previous assessments of land degradation which compounded historical land degradation with what is happening now.** The data since 1981 indicate current trends but tell us nothing about the historical legacy. For many purposes, it is more important to

address on-going land degradation; much historical land degradation may be irreversible.

5. **As a quantitative measure of land degradation, loss of NPP has been calculated for those areas where *both* NPP and RUE are declining.** This is likely to be a conservative estimate since globally, NPP has increased over the period. Also, where NPP is increasing but RUE is declining, some process of land degradation may have begun that is reducing NPP but is not yet reflected in declining NPP.

6. By the same reasoning, **RUE should be used alone for *early warning* of land degradation, or a herald of improvement.** Where NPP is rising but RUE declining, some process of land degradation might be under way that is not yet reflected in declining NPP; it will remain undetected if we consider only those areas where both indices are declining. The reverse also holds true: we might forgo promising interventions that increase RUE but have not yet brought about increasing NPP.

7. **Long-term trends of NDVI derivatives are unsophisticated indicators of land degradation and improvement. The various kinds of land degradation and improvement are not distinguished but as a proxy, NDVI/NPP trend does provide a globally consistent yardstick, and it does highlight places where biologically significant change is happening.** And this is its purpose: in the parent LADA program, this global scan will be used to direct attention to areas that demand investigation and action on the ground.

Acknowledgements

This work is part of the GEF/UNEP/FAO project *Land Degradation Assessment in Drylands*.

We thank CJ Tucker, JE Pinzon and ME Brown for access to the GIMMS dataset; J Grieser for providing the VASClimO precipitation data and M Salmon for providing the CRU TS climatic data; we are indebted to A Anyamba, R Biancalani, F Nachtergaele, SG Prince, BGJS Sonneveld, A Tengberg, GWJ van Lynden, P Vlek, and KJ Wessels for critical review; to P Tempel for help with data handling, and to YGL Karpes-Liem for text layout.

References

Alexandrov GA & T Oikawa 1997 Contemporary variations in terrestrial net primary productivity: the use of satellite data in the light of the extremal principle. *Ecological Modelling* 95, 113-118

Anyamba A & CJ Tucker 2005 Analysis of Sahelian vegetation dynamics using NOAA-AHVRR NDVI data from 1981-2003. *Journal of Arid Environments* 63, 596-614

Asrar GM, M Fuchs, ET Kanemasu & JL Hatfield 1984 Estimating absorbed photosyntheticaly active radiation and leaf area index from spectral reflectance in wheat. *Journal of Agronomy* 87, 300-306

Bai ZG & Dent DL 2006 *Global assessment of land degradation and improvement: pilot study in Kenya.* Report 2006/01, ISRIC - World Soil Information, Wageningen

Bai ZG & DL Dent 2007a *Land degradation and improvement in South Africa 1. Identification by remote sensing.* Report 2007 /03, ISRIC – World Soil Information, Wageningen

Bai ZG & DL Dent 2007b *Land degradation and improvement in Cuba 1. Identification by remote sensing.* Report 2007/04, ISRIC – World Soil Information, Wageningen

Bai ZG & DL Dent 2007c *Land degradation and improvement in China 1. Identification by remote sensing.* Report 2007/06, ISRIC – World Soil Information, Wageningen

Bai ZG & DL Dent 2007d *Land degradation and improvement in Argentina 1. Identification by remote sensing.* Report 2007/05, ISRIC – World Soil Information, Wageningen

Bai ZG & DL Dent 2007e *Land degradation and improvement in Senegal 1. Identification by remote sensing.* Report 2007/07, ISRIC – World Soil Information, Wageningen

Bai ZG & DL Dent 2007f *Land degradation and improvement in Tunisia 1. Identification by remote sensing.* Report 2007/08, ISRIC – World Soil Information, Wageningen

Bai ZG 2006 *Assessing land degradation in the Chittagong Hill Tracts, Bangladesh, using NASA GIMMS.* Report 2006/6, ISRIC – World Soil Information, Wageningen

Bai ZG, Dent DL. & Schaepman ME 2005 *Quantitative global assessment of land degradation and improvement: pilot study in North China.* Report 2005/6, ISRIC – World Soil Information, Wageningen

Beck C, J Grieser & B Rudolf 2005 A new monthly precipitation climatology for the global land areas for the period 1951-2000. 181-190 in *Climate Status Report 2004.* German Weather Service, Offenbach

Brown ME, JE Pinzon & K Didan 2006 Evaluation of the consistency of long-term NDVI time series derived from AVHRR, SPOT-Vegetation, SeaWIFS, MODIS and Landsat ETM+. *IEEE Transactions Geoscience Remote Sensing* 44, 1787-1793

CEISIN 2007 Socioeconomic Data Applications Center, Center for International Earth Science Information Network, Columbia University, Palisades NY http://sedac.ciesin.columbia.edu/gpw; http://sedac.ciesin.columbia.edu/povmap/ds_global.html (Accessed October10, 2007)

Chen S & P Rao 2008 Land degradation monitoring using multi-temporal Landsat TM/ETM data in a transition zone between grassland and cropland of northeast China. *International Journal of Remote Sensing* doi: 10.1080/01431160701355280.

CIESIN 2004 *Global Rural-urban mapping project: urban/rural extents.* Center for International Earth Science Information Network, Columbia Univ., Palisades NY

Engelen VWP van & TT Wen 1995 *Global and national soils and terrain databases (SOTER). Procedures manual (revised edition).* UNEP-FAO-ISRIC, Wageningen

FAO 2006 *Global forest resources assessment 2005.* Forestry paper 147 FAO, Rome

Fensholt R, I Sandholt & MS Rasmussen 2004 Evaluation of MODIS LAI, fAPAR and the relation between fAPAR and NDVI in a semi-arid environment using in situ measurements. *Remote Sensing of Environment* 91, 490-507

Fensholt R, I Sandholt, MS Rasmussen, S Stison & A Diouf 2006 Evaluation of satellite-based primary production modelling in the semi-arid Sahel. *Remote Sensing of the Environment* 105 173-188

Gebremichael M & AP Barros 2006 Evaluation of MODIS gross primary productivity (GPP) in tropical monsoon regions. *Remote Sensing of Environment* 100, 150–166

Hall F, J Masek & GJ Collatz 2006 Evaluation of ISLSCP Initiative II FASIR and GOMMS NDVI products and implications for carbon cycle science. *Journal of Geophysical Research* 111: D22S08 doi:10.1029/2006JD007438

Holm AMS, W Cridland & ML Roderick 2003 The use of time-integrated NOAA NDVI data and rainfall to assess landscape degradation in the arid shrubland of Western Australia. *Remote Sensing of Environment* 85, 145-158

Houérou HN le 1984 Rain-use efficiency: a unifying concept in arid-land ecology. *Journal of Arid Environments* 7, 213-247

Houérou HN le, RL Bingham & W Skerbek 1988 Relationship between the variability of primary production and variability of annual precipitation in world arid lands. *Journal of Arid Environments* 15, 1-18

Houghton RA 2008 Carbon flux to the atmosphere from land use changes 1850-2005. *TRENDS: A compendium of data on global change.* Carbon Dioxide Information Analysis Center, Oak Ridge National Laboratory, US Dept Energy, Oak Ridge TE http://cdiac.oml.gov/trends/landuse/hughton.html Accessed 13 May 2008

Illius AW and TG O'Connor 1999 On the relevance of nonequilibrium concepts to arid and semiarid grazing systems. *Ecological Applications* 9, 798–813

IPCC 2000 Global perspective. 25-51 In: Watson RT, IR Noble, B Bolin and others (editors) *Land use, land-use change, and forestry.* Published for the Intergovernmental Panel on Climate Change by Cambridge University Press, Cambridge

ISRIC 2008 a *Global SOTER landform classification scale 1:1 million.* ISRIC Working Paper, Wageningen

ISRIC 2008b *Enhanced soil information for LADA partner countries, scale 1:1million. ISRIC* Working Paper, Wageningen

Jones JAA 1997 *Global hydrology: processes, resources and environmental management.* Longman, Harlow

JRC 2003 *Global Land Cover 2000 database.* European Commission, Joint Research Centre, http://www-gem.jrc.it/glc2000. Accessed February 2, 2007

Justice CO, JRG Townshend, EF Vermote and others 2002 An overview of MODIS Land data processing and product status. *Remote Sensing of Environment* 83, 3-15

Justice CO, G Dugdale, JRG Townshend and others 1991 Synergism between NOAAAVHRR and Meteosat data for studying vegetation development in semi-arid West Africa. *International Journal of Remote Sensing* 12, 1349–1368

Kurz WA, CC Dymond, G Stinson and others 2008 Mountain pine beetle and forest carbon feedback to climate change. *Nature* 452, 24, 987 doi: 10.1038/nature06777

Livezy RE & WY Chen 1983 Statistical field significance and its determination by Mote Carlo techniques. *Monthly Weather Review* 111, 46-59

Mitchell TD & PD Jones 2005 An improved method of constructing a database of monthly climate observations and associated high-resolution grids. *International Journal of Climate* 25, 693-712

Monbiot G 2008 It makes economic sense to kill people. *The Guardian Weekly* 20.02.08, page 19

Myneni RB, R Ramakrishna, R Nemani & S Running 1997 Estimation of global leaf area index and absorbed PAR using radiative transfer models. *IEEE Transactions Geoscience Remote Sensing* 35 1380-1393

Nemani RR, CD Keeling, H Hashimoto and others 2003 Climate-driven increases in global terrestrial net primary production from 1982 to 1999. *Science* 300, 1560-1563

O'Connor TG, LM Haines & HA Snyman 2001 Influence of precipitation and species composition on phytomass of a semi-arid African grassland. *Journal of Ecology* 89, 850-860

Oldeman LR, RTA Hakkeling & WG Sombroek 1991. *World map of the status of human-induced soil degradation, 2nd edition.* ISRIC, Wageningen

Olsson L, L Eklundh & J Ardö 2005. A recent greening of the Sahel – trends, patterns and potential causes. *Journal of Arid Environments* 63, 556-566

Plummer S 2006 On validation of the MODIIS gross primary production product. *IEEE Transactions on Geoscience and Remote Sensing* 44, 7, 1936-1938

Prince SD, KJ Wessels, CJ Tucker & SE Nicholson 2007 Desertification in the Sahel: a reinterpretation of a reinterpretation. *Global Change Biology* 13, 1308-1313

Rasmussen MS 1998a Developing simple, operational, consistent NDVI-vegetation models by applying environmental and climatic information Part II: Crop yield assessment. *International Journal of Remote Sensing* 19, 119-139

Rasmussen MS 1998b Developing simple, operational, consistent NDVI-vegetation models by applying environmental and climatic information: Part I: Assessment of net primary production. *International Journal of Remote Sensing* 19, 97-117

Ripple WJ 1985 Asymptotic reflectance characteristics of grass vegetation. *Photogrammetric Engineering Remote Sensing* 51, 1915-1921

Running SW, FA Heinsch, M Zhao, M Reeves & H Hashimoto 2004 A continuous satellite-derived measure of global terrestrial production. *Bioscience* 54, 547-560

Seaquist JW, L Olsson & J Ardö 2003 A remote sensing-based primary production model from grassland biomes. *Ecological Modelling* 169, 131-155

Snyman HA 1998 Dynamics and sustainable utilization of rangeland ecosystems in arid and semi-arid climates of southern Africa. *Journal of Arid Environments* 39, 645–666

Sonneveld BGJ. & DL Dent 2007 How good is GLASOD? *Journal of Environmental Management* doi:10.1016/j.jenvman.2007.09.008

Thornton PE, Running SW & Hunt ER 2005 *Biome-BGC: Terrestrial Ecosystem Process Model, Version 4.1.1.* Oak Ridge National Laboratory Distributed Active Archive Center, Oak Ridge TE http://www.daac.ornl.gov

TRMM 2008. http://trmm.gsfc.nasa.gov/, accessed May 1, 2008

Tucker CJ, JE Pinzon & ME Brown 2004 *Global Inventory Modeling and Mapping Studies (GIMMS) satellite drift corrected and NOAA-16 incorporated normalised difference vegetation index (NDVI), monthly1981-2002.* University of Maryland

Turner DP, WD Ritts, WB Cohen and others 2003 Scaling gross primary production (GPP) over boreal and deciduous forest landscapes in support of MODIS GPP product validation. *Remote Sensing of Environment* 88, 256–270

Turner DP, WD Ritts, WB Cohen and others 2006 Evaluation of MODIS NPP and GPP products across multiple biomes. *Remote Sensing of Environment* 102, 282–292

UNCED 1992 Managing fragile ecosystems: combating desertification and drought Agenda 21, Chapter 12 United Nations Conference on Environment and Development http://wwwunorg/esa/sustdev/documents/agenda21. Accessed August 5, 2005

UNEP 2007 *Global Environmental Outlook GEO-4*, UN Environment Programme, Nairobi

WaterWatch 2008 http://www.WaterWatch.nl accessed May 1, 2008

Wessels KJ, SD Prince, J Malherbe and others 2007 Can human-induced land degradation be distinguished from the effects of rainfall variability? A case study in South Africa. *Journal of Arid Environments* 68, 271-297

Wessels KJ, SD Prince, PE Frost & D VanZyl 2004 Assessing the effects of human-induced land degradation in the former homelands of northern South Africa with a 1-km AVHRR NDVI time-series. *Remote Sensing and Environment 91, 47-67*

Wit de A 2004 The IDL-ENVI implementation of the HANTS algorithm (personal communication)

Zhao M, FA Heinsch, RR Nemani & SW Running 2005 Improvements of the MODIS terrestrial gross and net primary production global data set. *Remote Sensing of Environment* 95, 164-176

Zhao M, SW Running & RR Nemani 2006 Sensitivity of Moderate Resolution Imaging Spectroradiometer (MODIS) terrestrial primary production to the accuracy of meteorological reanalyses. *Journal of Geophysical Research* 111, G01002, doi:10.1029/2004JG000004

Appendix 1: Data

Table S1 GLASOD estimates of human-induced soil degradation, million ha

Kind of degradation	World	Asia	West Asia	Africa	Latin America and Caribbean	North America	Australia and Pacific	Europe
Water erosion	1094	440	84	227	169	60	83	115
Wind erosion	548	222	145	187	47	35	16	42
Nutrient depletion	135	15	6	45	72	-	+	3
Salinity	76	53	47	15	4	-	1	4
Contamination	22	2	+	+	+	-	-	19
Physical	79	12	4	18	13	1	2	36
Other	10	3	1	2	1	-	1	2
Sum	1964	747	287	494	306	96	103	218

GLASOD, reporting in 1991, indicated that 15 per cent of land was degraded. The highest proportions were reported for Europe (25 per cent), Asia (18 per cent) and Africa (16 per cent); the least in North America (5 per cent). By the same measure, as a proportion of the degraded area, soil erosion affected 83 per cent of the global degraded area (ranging from 99 per cent in North America to 61 per cent in Europe); nutrient depletion affected 4 per cent globally but 28 per cent in South America; salinity less than 4 per cent worldwide but 16 per cent in West Asia; chemical contamination about 1 per cent globally but 8 per cent in Europe; soil physical problems 4 per cent globally but 16 per cent in Europe.

Table S2 Statistics of NDVI indicators*

NDVI indicators	NDVI values			Pixels (%)		% NDVI change/year			Δ NDVI/year		
	min	max	mean	Pos.	Neg.	Pos.	Neg.	mean	Pos.	Neg.	mean
Minimum	0.132	0.296	0.182	59.5	40.5	0.966	0.851	0.232	0.0019	0.0014	0.00055
Maximum	0.527	0.716	0.622	50.5	49.5	0.391	0.260	0.060	0.0019	0.0017	0.00014
Max-Min	0.322	0.575	0.443	46.0	54.0	0.732	0.670	-0.036	0.0023	0.0026	-0.00039
Mean	0.314	0.411	0.365	67.6	32.4	0.368	0.245	0.164	0.0011	0.0009	0.00043
Sum	3.762	4.932	4.383	67.6	32.4	0.368	0.245	0.164	0.0129	0.0104	0.00518
STD	0.110	0.192	0.150	53.2	46.8	0.707	0.684	0.046	0.0008	0.0008	0.00005
CoV	0.206	0.394	0.294	41.5	58.5	0.772	0.735	-0.113	0.0036	0.0033	-0.00044

*In the calculations of the min., max. and mean values of each NDVI indicator, an average value of the all pixels in the vegetated area, defined as areas with net primary productivity greater than 1 g C m-2 year-1, were calculated. For example, min. value of the Maximum NDVI indicator: overlay statistic minimum of CELL STATISTIC in ArcMap was performed to extract minimum values of the time series annual Maximum NDVI for each pixel over the period (1981-2003), and the averaged minimum value of the maximum NDVI for all pixels was assigned as min. for the Maximum NDVI indicator; max. value of the Maximum NDVI indicator: overlay statistic maximum of CELL STATISTIC in ArcMap was performed to extract maximum values of the time series annual Maximum NDVI for each pixel over the period (1981-2003), and the averaged maximum value of the maximum NDVI for all pixels was assigned as max. for the Maximum NDVI indicator; mean value of the Maximum NDVI indicator: overlay statistic mean of CELL STATISTIC in ArcMap was performed to extract mean values of the time series annual Maximum NDVI for each pixel over the period (1981-2003), and the averaged mean value of the maximum NDVI for all pixels was assigned as mean for the Maximum NDVI indicator.

The rates of the positive and negative pixels were counted from the slope of the regression, i.e., positive slope (pos.) negative slope (neg.).

% NDVI change/year was calculated from the trend maps for each NDVI indicator: positive value (pos.) is the average of the all pixels with a positive trend; negative (neg.) is the average of the all pixels with a negative trend; mean value is the average of the all pixels; Δ NDVI/year is calculated the same as % NDVI change but from the absolute change maps.

Appendix 2: Analytical methods

Derivation of NDVI indicators

ArcGIS Spatial Analyst, ERDAS IMAGINE and ENVI-IDL were used to calculate NDVI minimum, maximum, maximum-minimum, mean, sum, standard deviation, and coefficient of variation (Appendix 3), as well as climate variables. The fortnightly NDVI data were geo-referenced and averaged to monthly; annual NDVI indicators (for the calendar year in the northern hemisphere and from 1 October to following 30 September for the southern hemisphere) were derived for each pixel; their temporal trends were determined by linear regression at an annual interval and mapped to depict spatial changes.

A negative slope of linear regression indicates a decline of green biomass and a positive slope, an increase – except for STD and CoV which indicate trends in variability. The absolute change (Δ in map legends, titled "changes in …..") is the slope of the regression; the relative change (% in map legends, titled "trend in ….") is 100(slope of the regression/multi-year mean).

Monthly grids of rainfall for the period 1981-2002 were geo-referenced and re-sampled to the same spatial resolution as the NDVI (8km) using neighbourhood statistics. Spatial pattern and temporal trend of rainfall and rain-use efficiency (RUE, the ratio of annual NDVI and annual rainfall) for each pixel were determined by regression.

Land degradation was identified by negative trends of both biomass and rain-use efficiency. To distinguish between declining productivity caused by land degradation, and declining productivity due to other factors, rainfall variability has been accounted for by, first, identifying pixels where there is a positive relationship between productivity and rainfall. Secondly, for those areas where productivity depends on rainfall, rain-use efficiency has been considered: where productivity declined but RUE increased, we attribute the decline of productivity to declining rainfall and those areas are masked.

Land improvement was identified by positive changes in sum NDVI, positive rain-use efficiency in those areas where there is which has a positive correlation between sum NDVI and rainfall and RUE, and positive energy-use efficiency.

Plots of both land degradation and land improvement were masked by the mapped urban extents

Statistical tests

The trend analysis assumes that the data are spatially and temporally independent. This was tested by examining autocorrelation coefficients following Livezy and Chen (1983). When the absolute values of the autocorrelation coefficients of lag-1 to lag-3 calculated for a time series consisting of *n* observations are not larger than the typical critical value corresponding to 5 per cent significance level, i.e., $1.96/\sqrt{n}$, the observations in this time series can be accepted as being independent from each other.

The T-test was used to arrange the slope values in classes showing strong or weak positive or negative trends:

$$T = b / se(b)$$

Where *b* is the calculated slope of the regression line between the observation values and time and *se(b)* represents the standard error of *b.*

The class boundaries were defined for 95 per cent confidence level; trends were labelled *high* if the *T*-values of the slope exceeded the 0.025 *p*-value of either tail of the distribution; lesser *T*- values were labelled *low*.

In addition, SPSS and MS Excel were employed to analyze trends, correlations and significances of the non-gridded variables.

Maps of the degrading areas or improving areas were overlaid on the other maps. Corresponding comparative values were calculated, pixel-by-pixel and a univariate correlation calculated.

Appendix 3: NDVI indicators of the land degradation / improvement

Minimum NDVI: The lowest value that occurs in any one year (annual) - which is usually at the end of the dry season. Variation in minimum NDVI may serve as a baseline for other parameters.

Maximum or peak NDVI: Represents the maximum green biomass. The large spatial variations reflect the diverse landscapes and climate.

Maximum-minimum NDVI: The difference between annual maximum and minimum NDVI reflects annual biomass productivity for areas with one, well-defined growing season but may not be meaningful for areas with bimodal rainfall.

Sum NDVI: The sum of fortnightly NDVI values for the year most nearly aggregates annual biomass productivity.

Standard deviation (STD): NDVI standard deviation is the root mean square deviation of the NDVI time series values (annual) from their arithmetic mean. It is a measure of statistical dispersion, measuring the spread of NDVI values.

Coefficient of variation (CoV): CoV can be used to compare the amount of variation in different sets of sample data. NDVI CoV images were generated by computing for each pixel the standard deviation (STD) of the set of individual NDVI values and dividing this by the mean (M) of these values. This represents the dispersion of NDVI values relative to the mean value.

Temporal trends: The long-term trends of the indicators of biological productivity may be taken as indicators of land degradation (where the trend is declining) or land improvement (where the trend is increasing). A positive change in the value of a pixel-level CoV over time relates to increased dispersion of values, not increasing NDVI; similarly, a negative CoV dispersion – which is the case over nearly the whole country - means decreasing dispersion of NDVI around mean values, not decreasing NDVI.

The patterns and trends of all NDVI indicators for each pixel, determined by the slope of the linear regression equation, are depicted in Figures S1-7; their values are summarised in Table S2. No further analyses were made for these indicators except for the sum NDVI which is discussed in detail in the main text. It is recommended, however, that these maps should be considered in the field investigation - in particular the land use change during the study period (1981-2003).

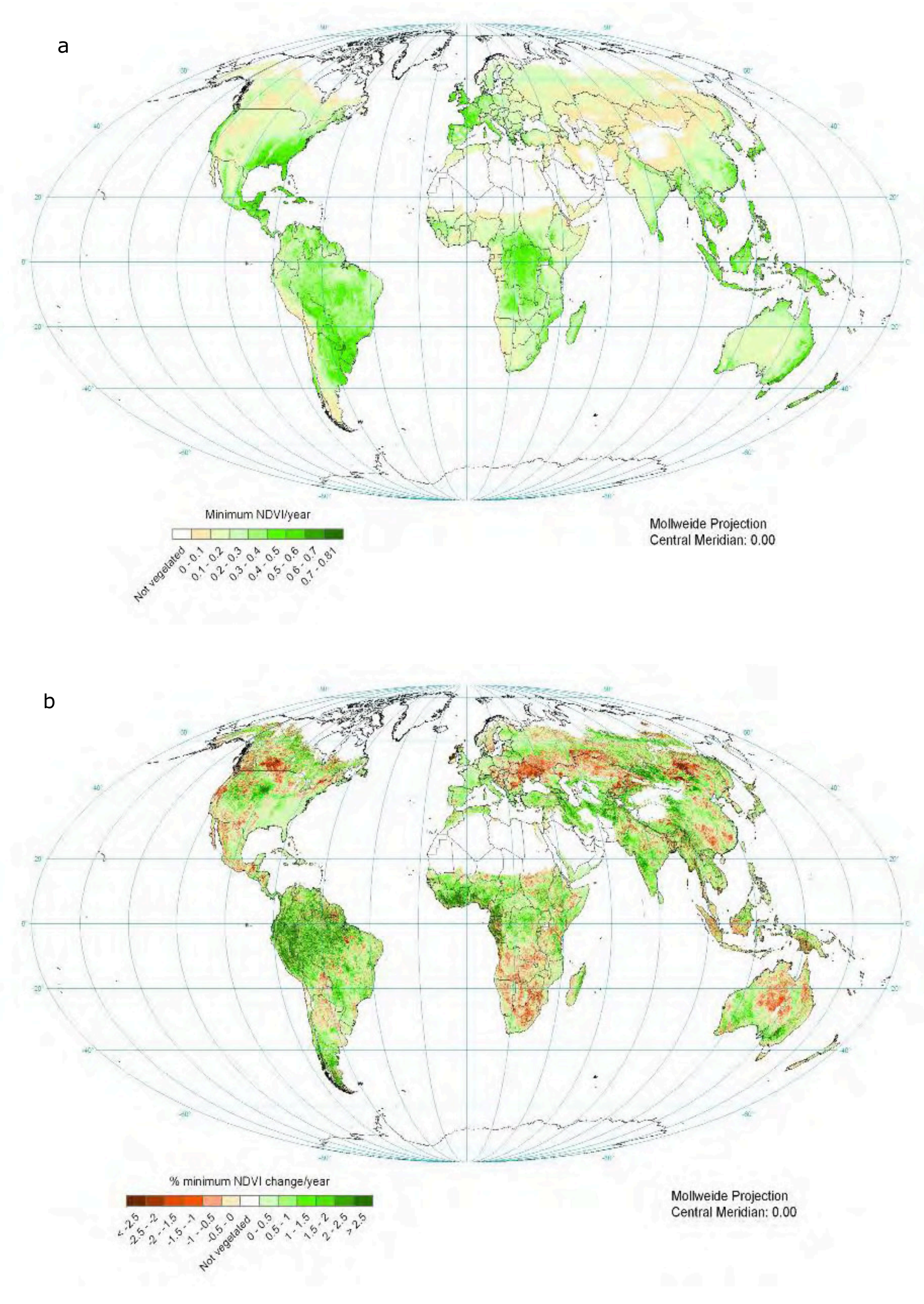

Figure S1. Annual minimum NDVI 1981-2003: Pattern (a), trends (b – percentage)

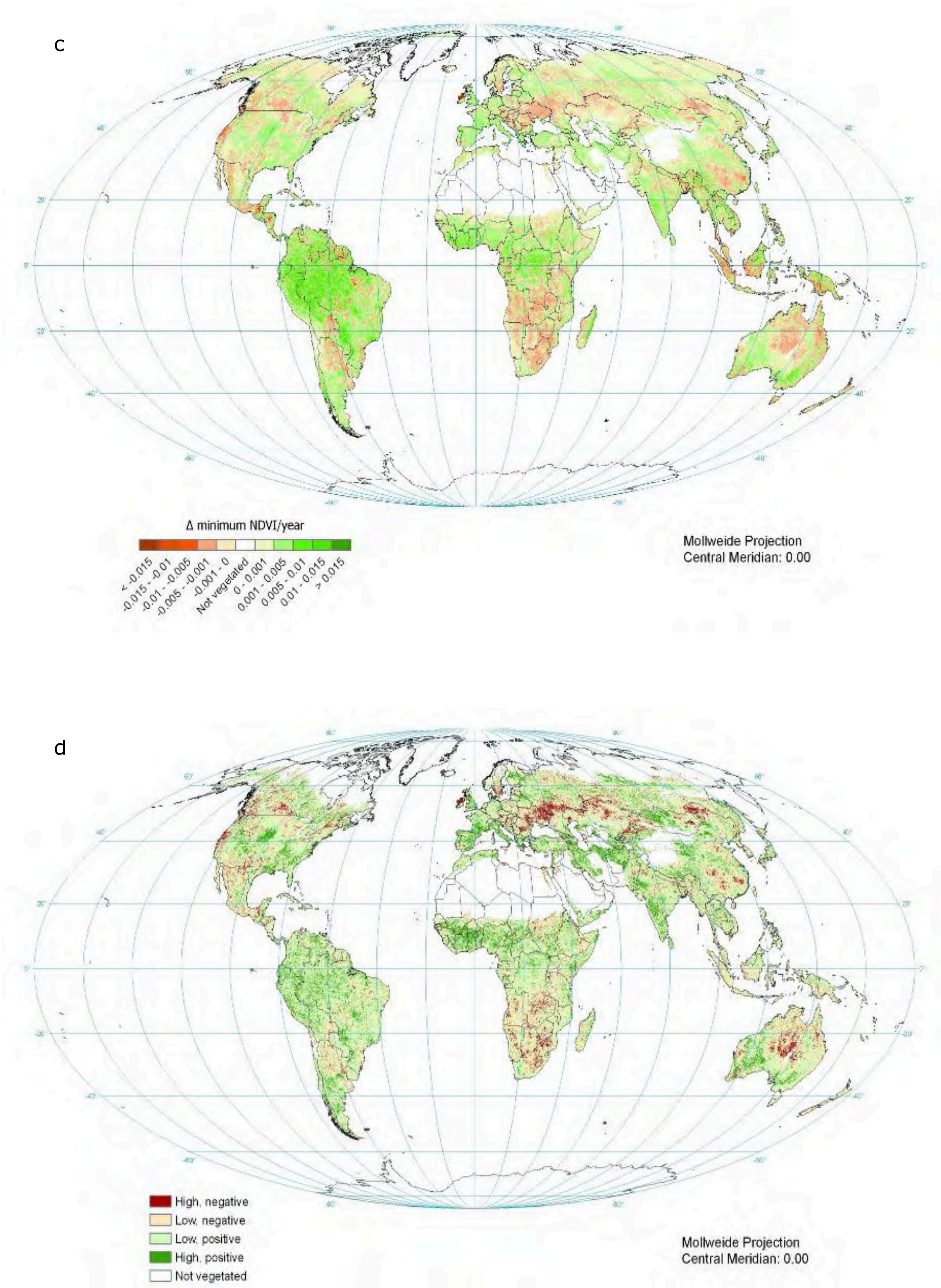

Figure S1. Annual minimum NDVI 1981-2003: Trend (c – absolute) and confidence levels (d)

a

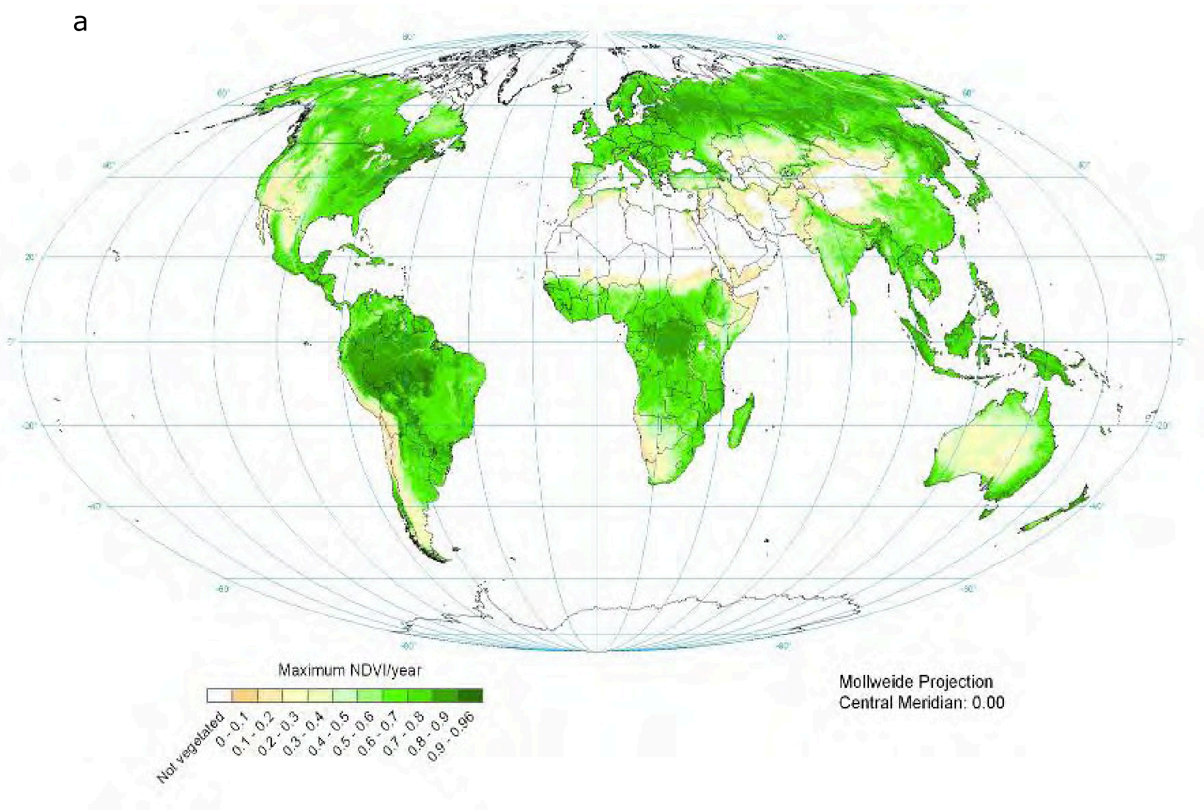

b

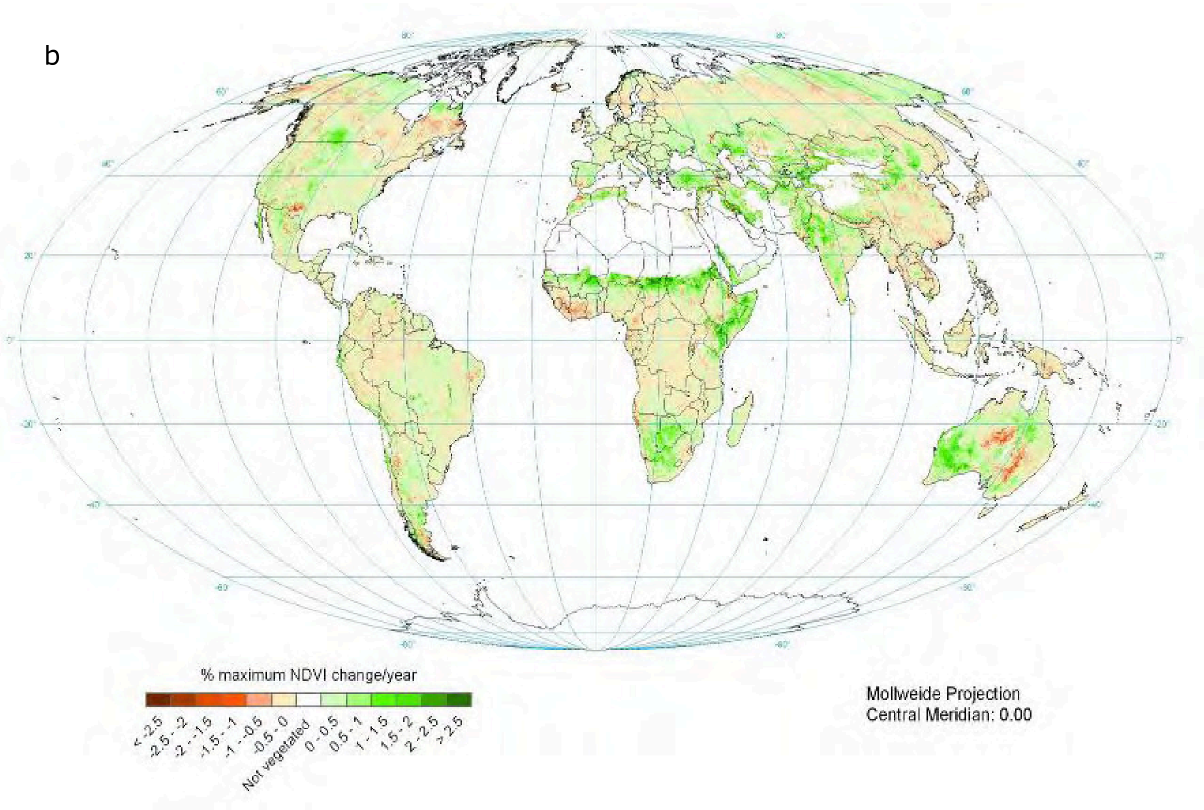

Figure S2. Annual maximum NDVI 1981-2003: Pattern (a), trends (b – percentage)

c

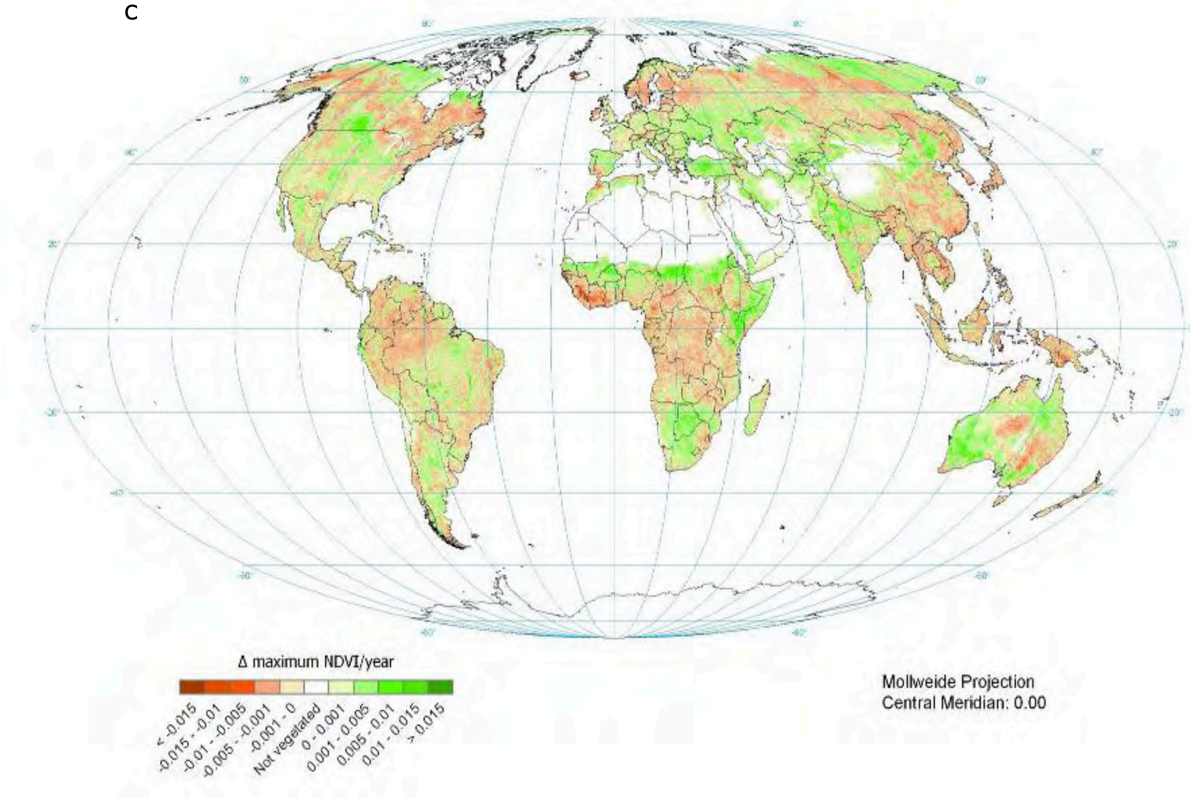

d

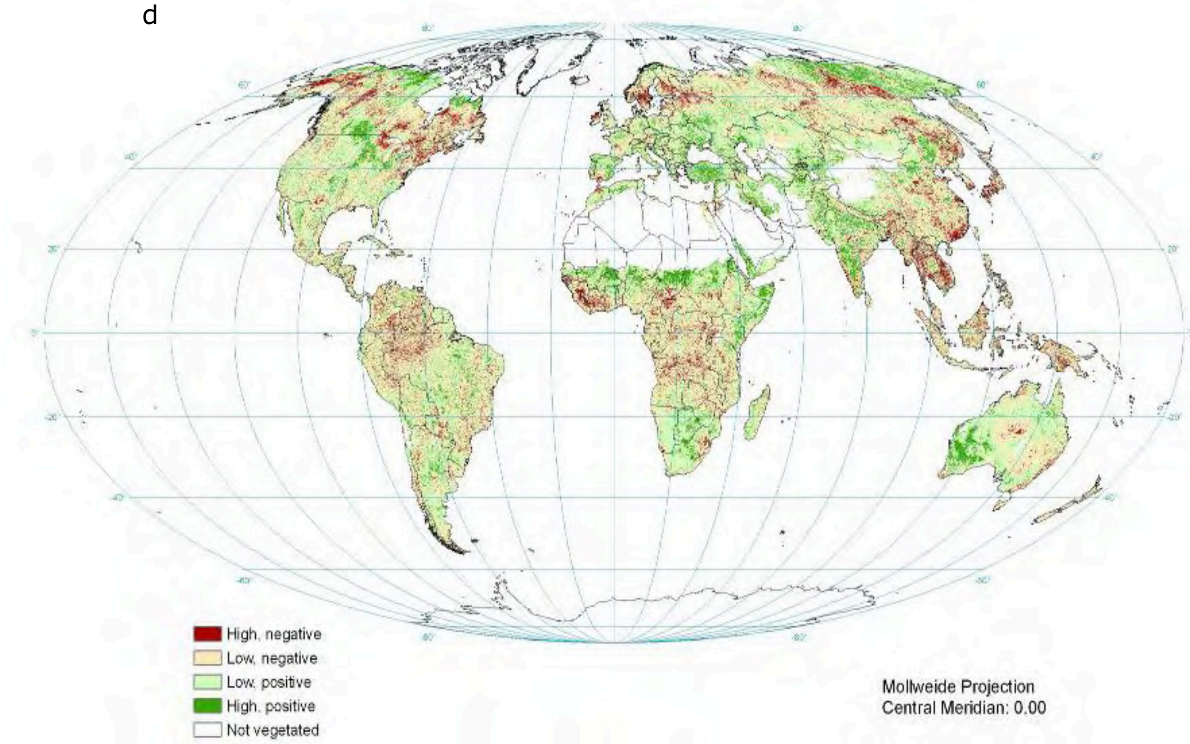

Figure S2. Annual maximum NDVI 1981-2003: Pattern (a), trends (c – absolute) and confidence levels (d)

a

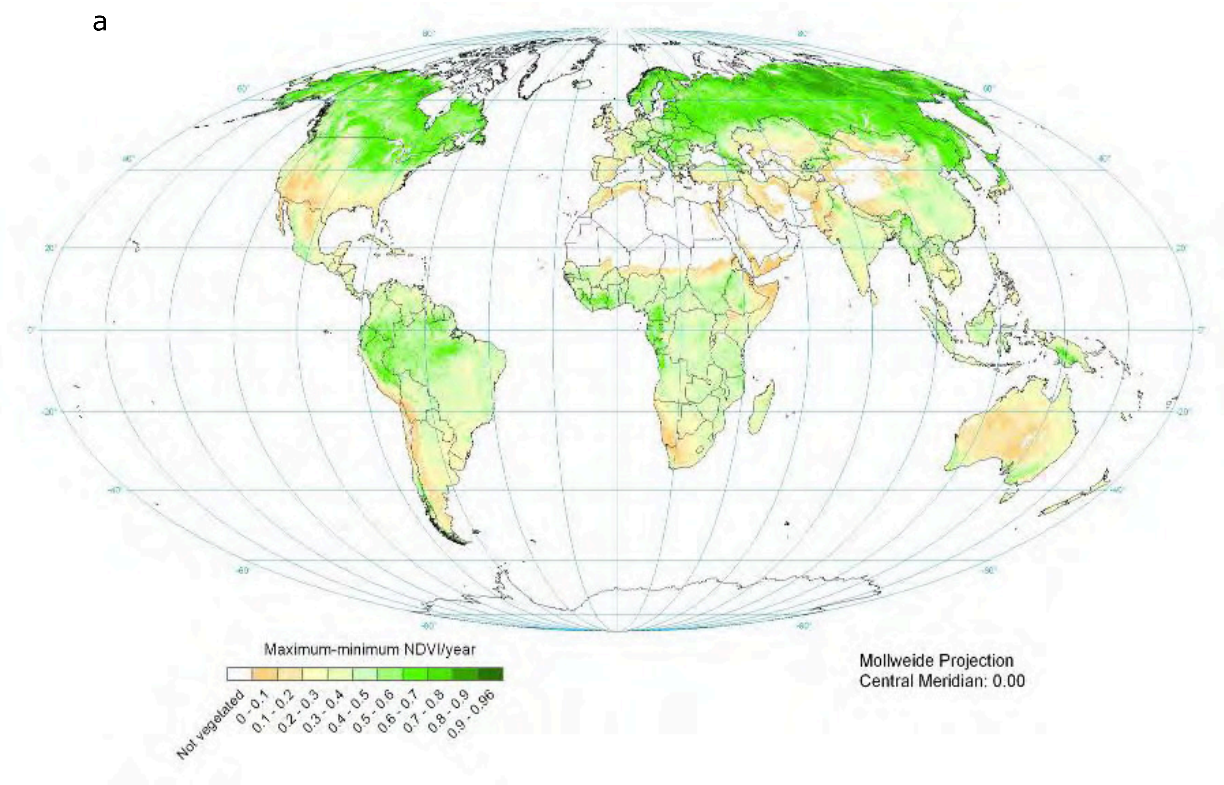

b

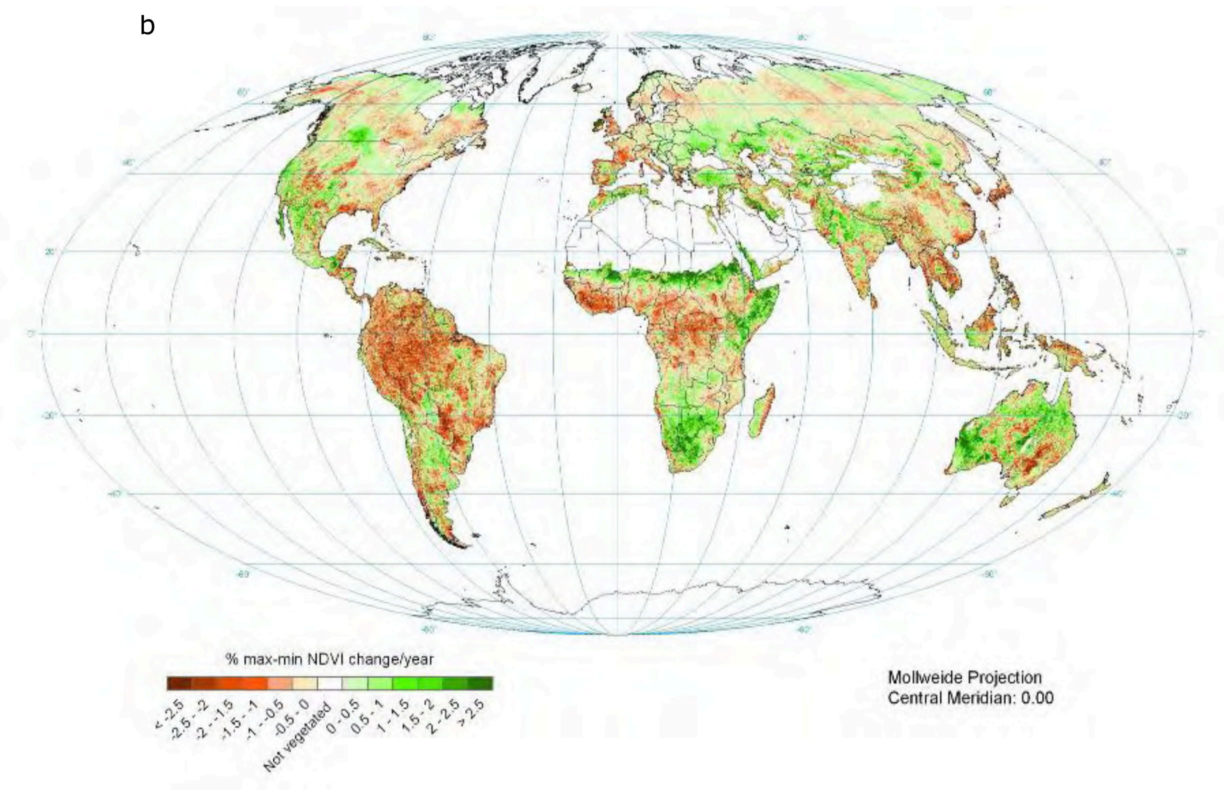

Figure S3. Annual max-min NDVI 1981-2003: Pattern (a), trends (b – percentage)

c

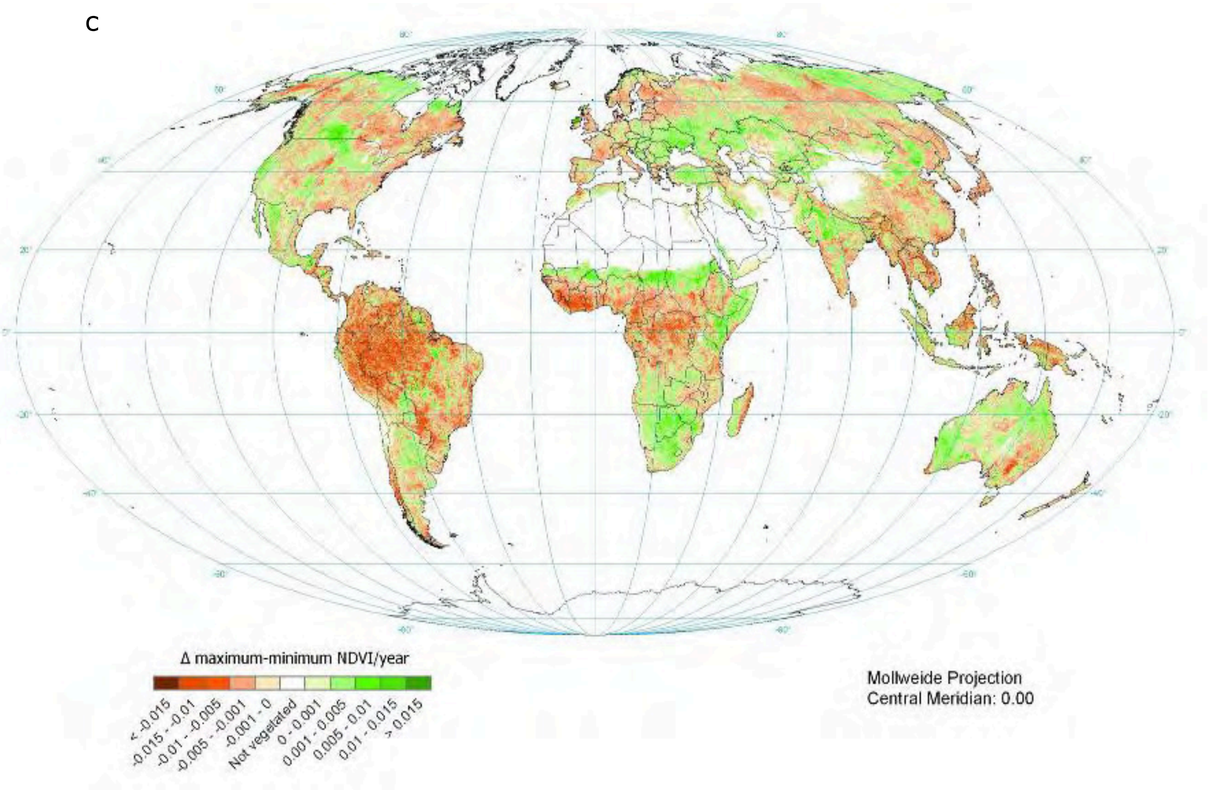

d

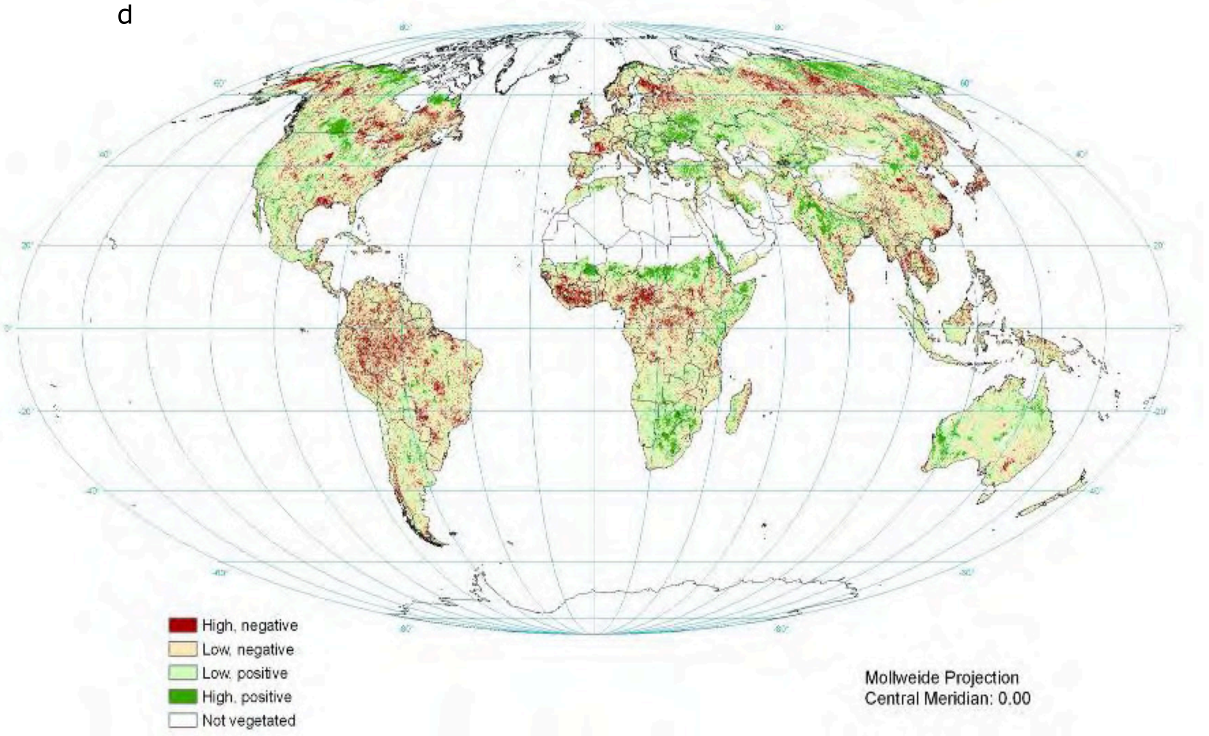

Figure S3. Annual max-min NDVI 1981-2003: trends (c – absolute) and confidence levels (d)

a

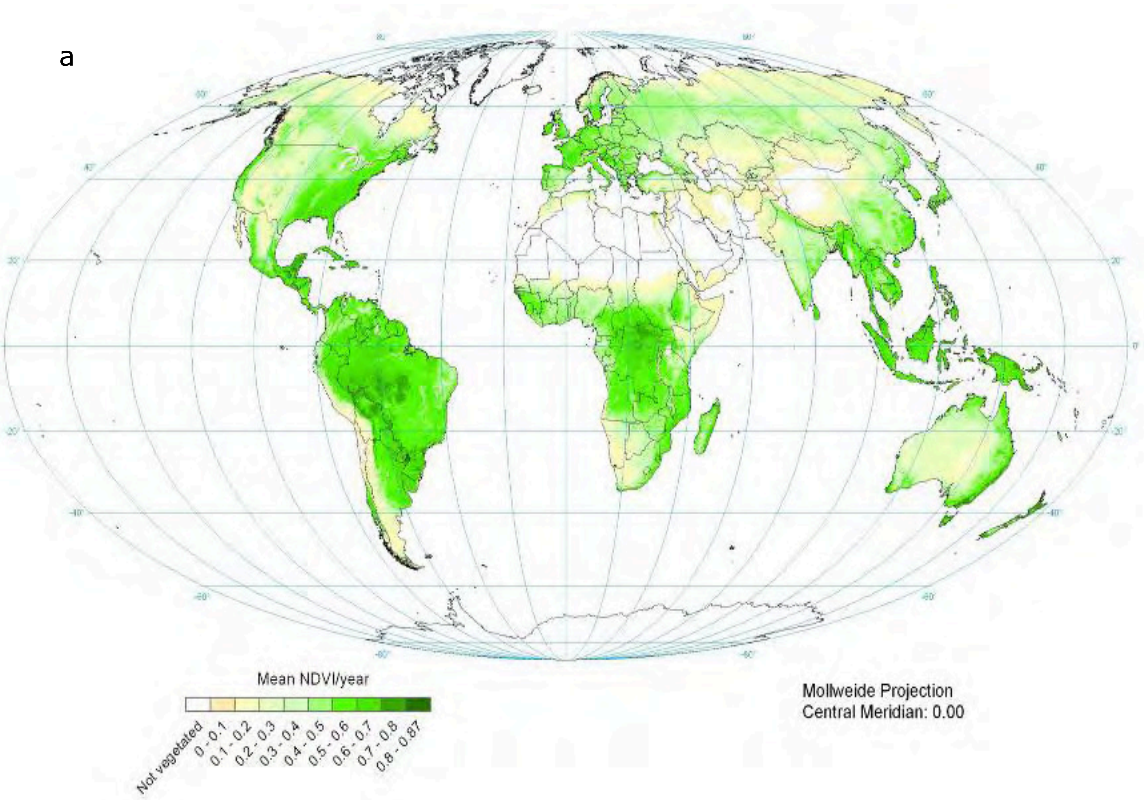

b

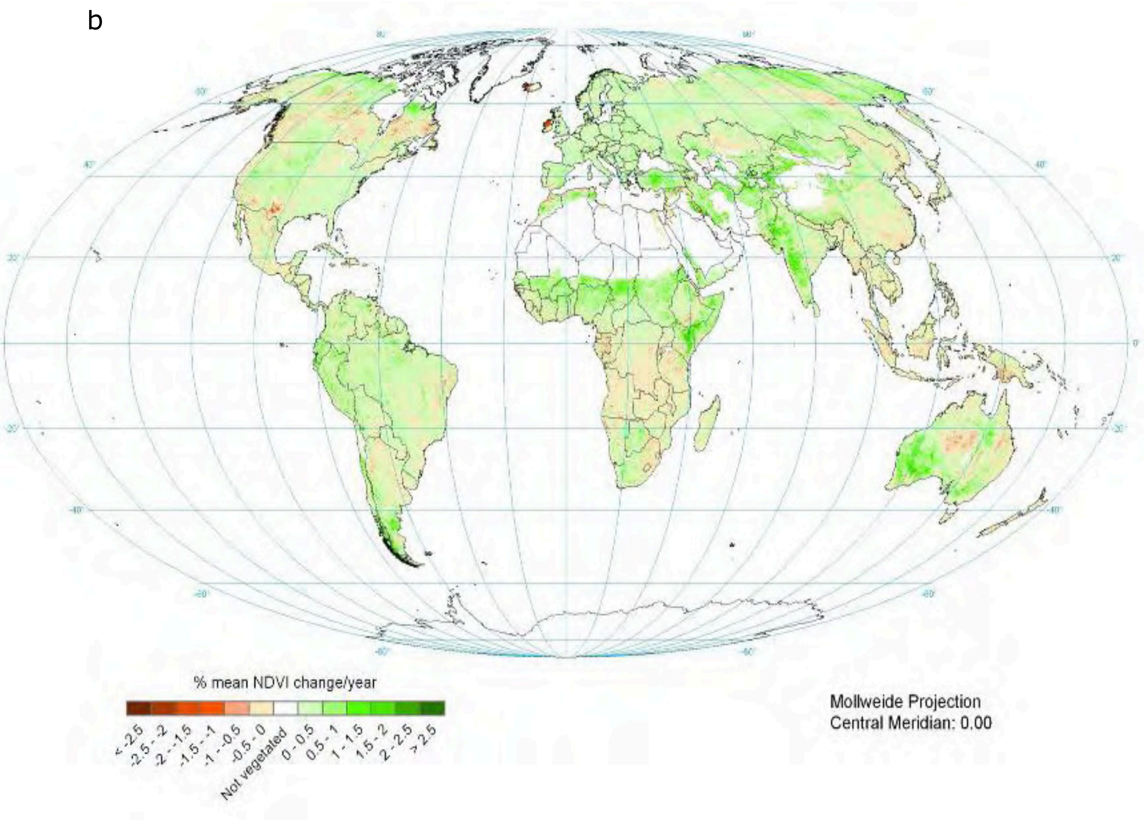

Figure S4. Annual mean NDVI 1981-2003: Pattern (a), trends (b – percentage)

c

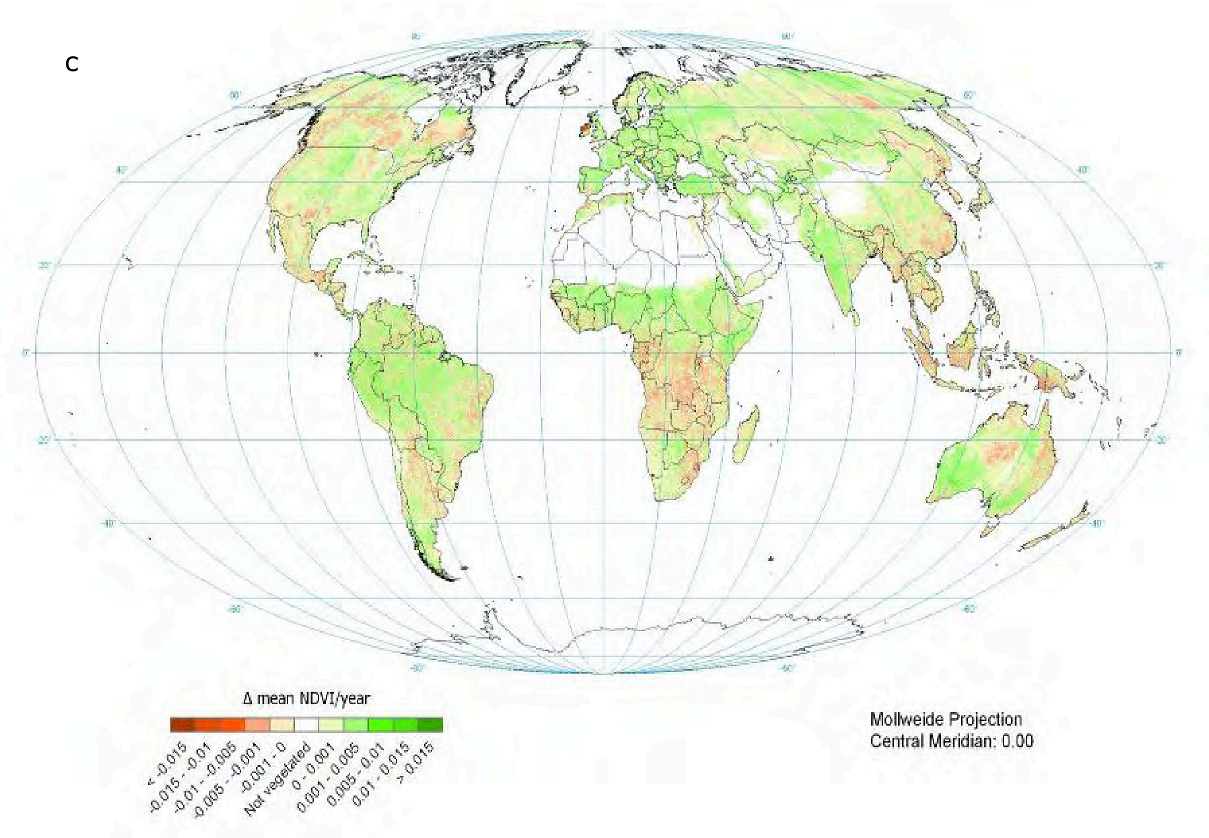

d

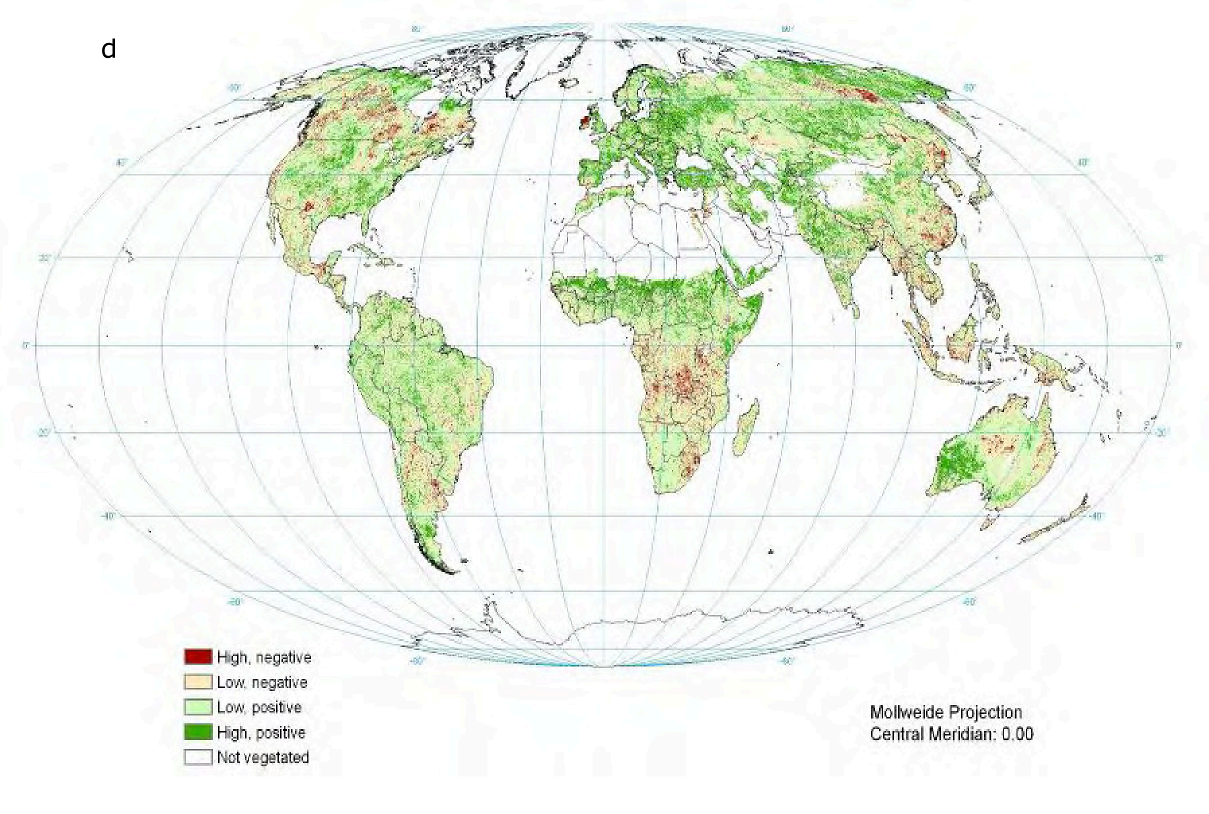

Figure S4. Annual mean NDVI 1981-2003: trends (c – absolute) and confidence levels (d)

a

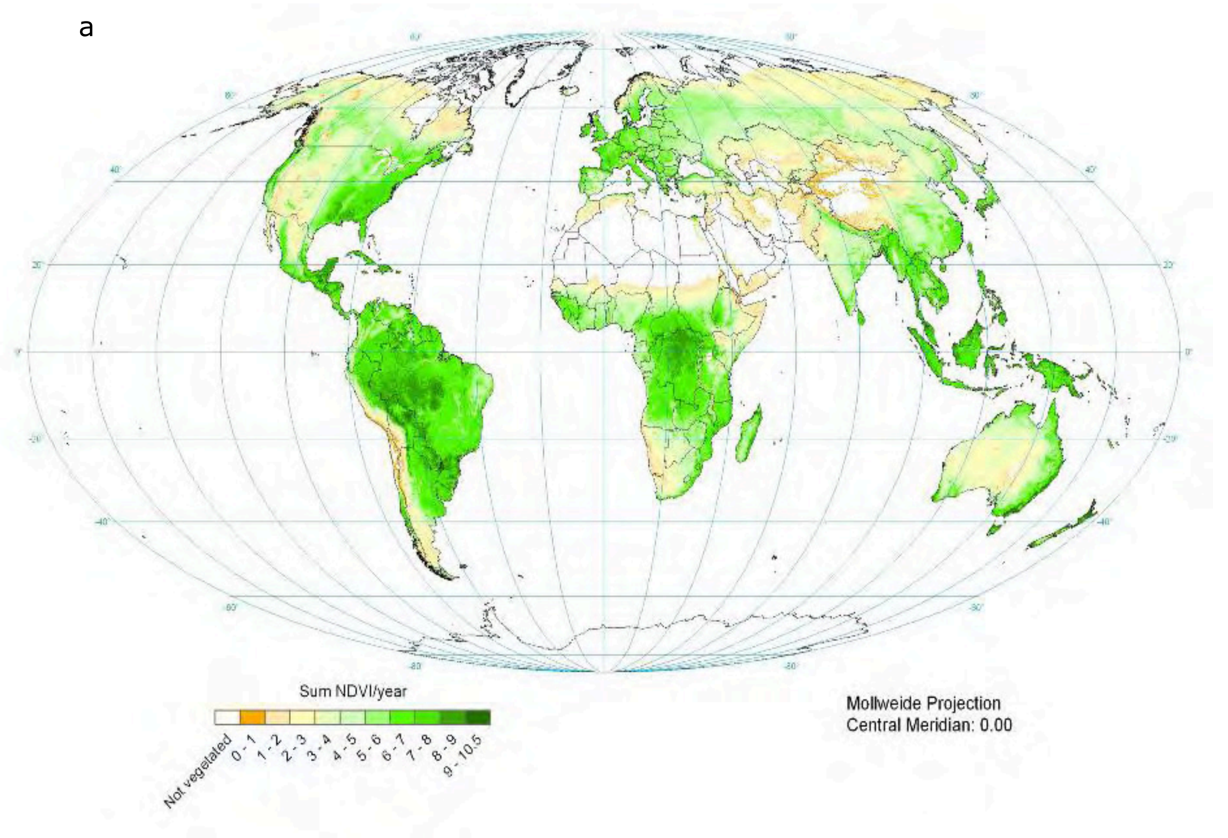

b

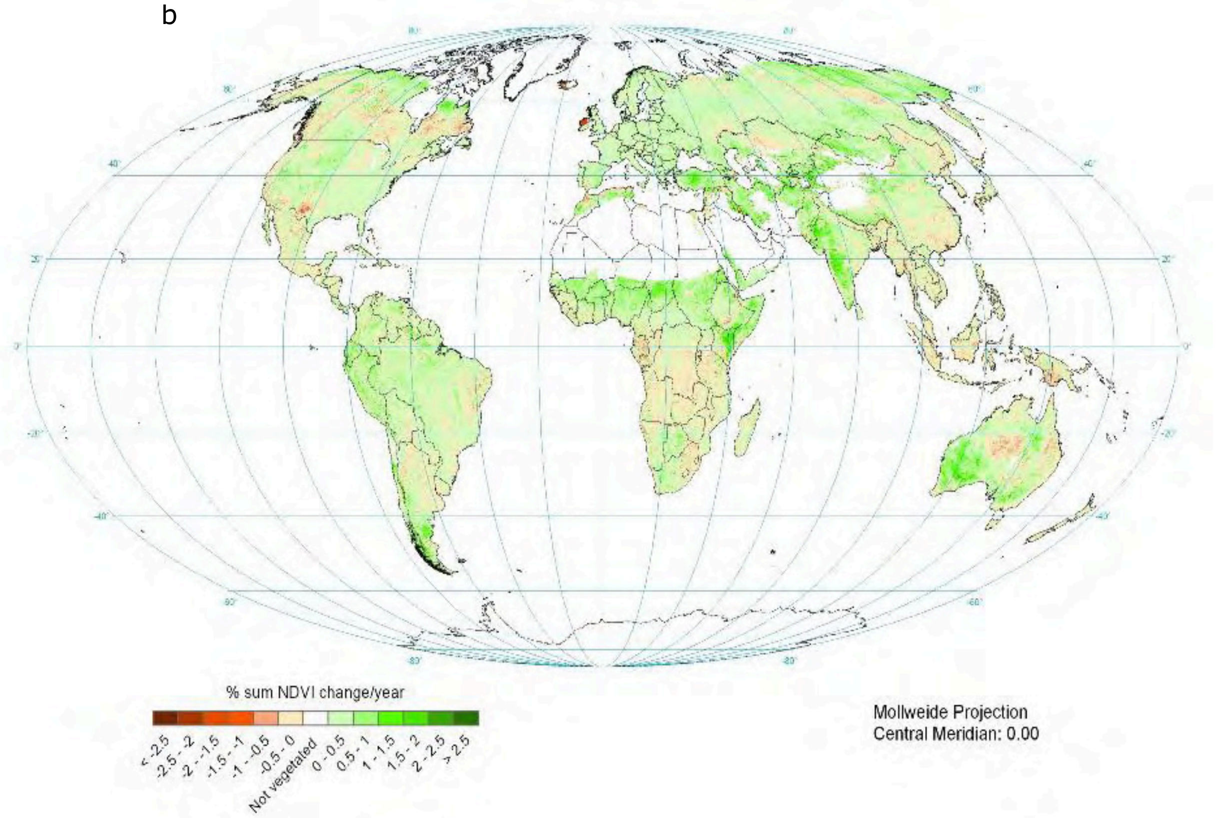

Figure S5. Annual sum NDVI 1981-2003: Pattern (a), trends (b – percentage)

c

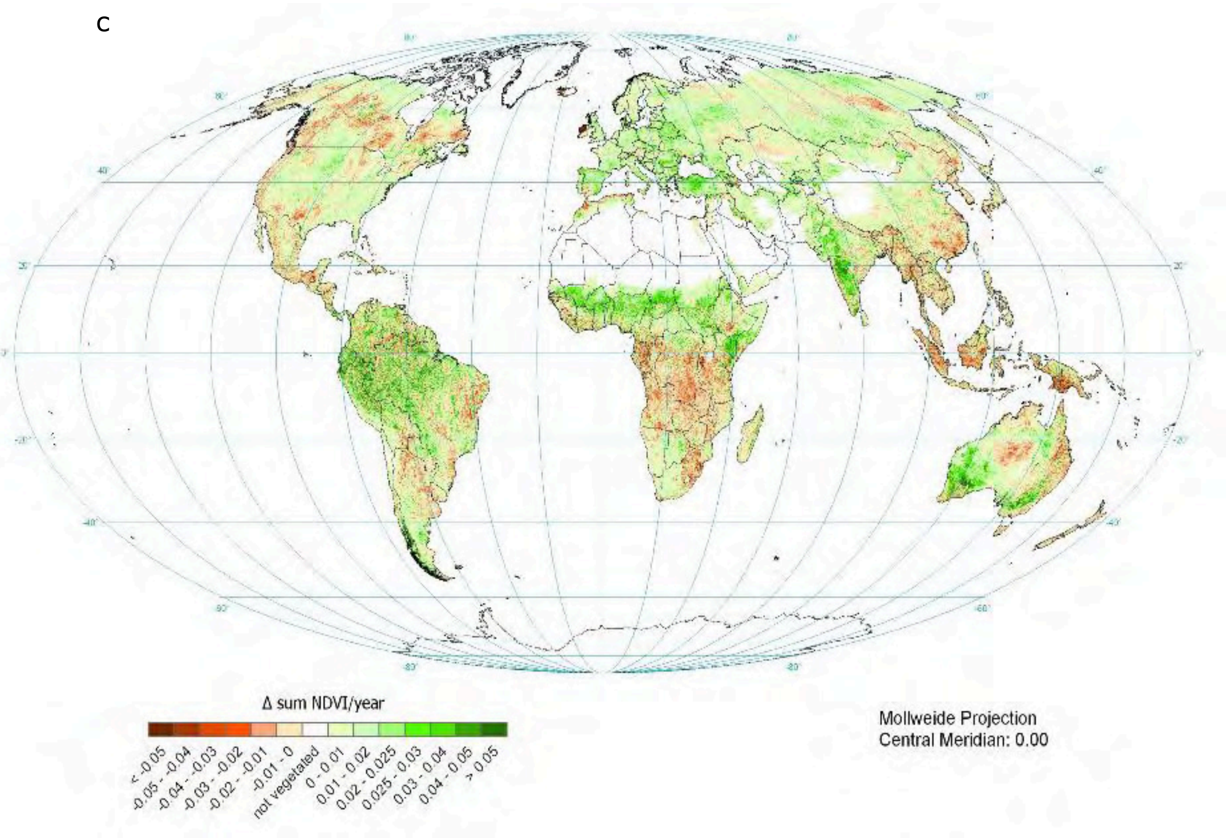

d

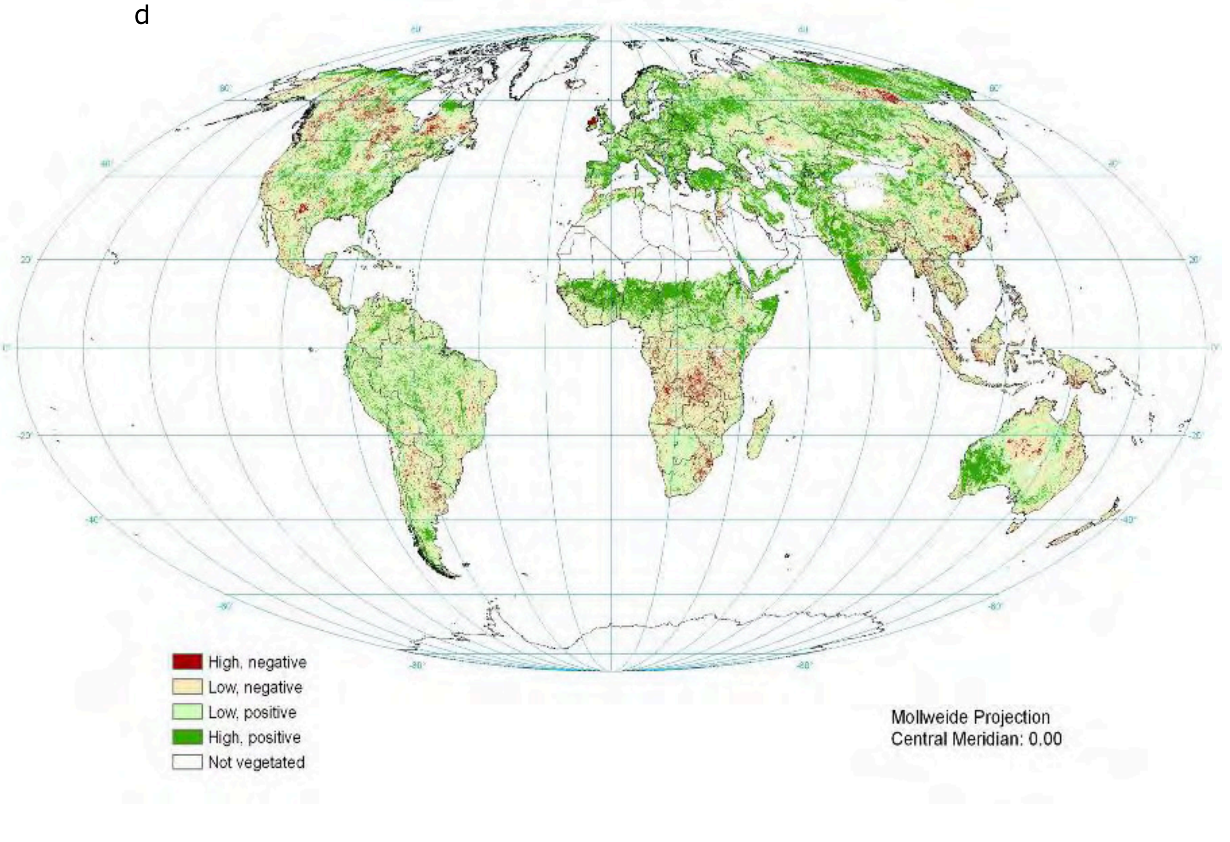

Figure S5. Annual sum NDVI 1981-2003: trends (c – absolute) and confidence levels (d)

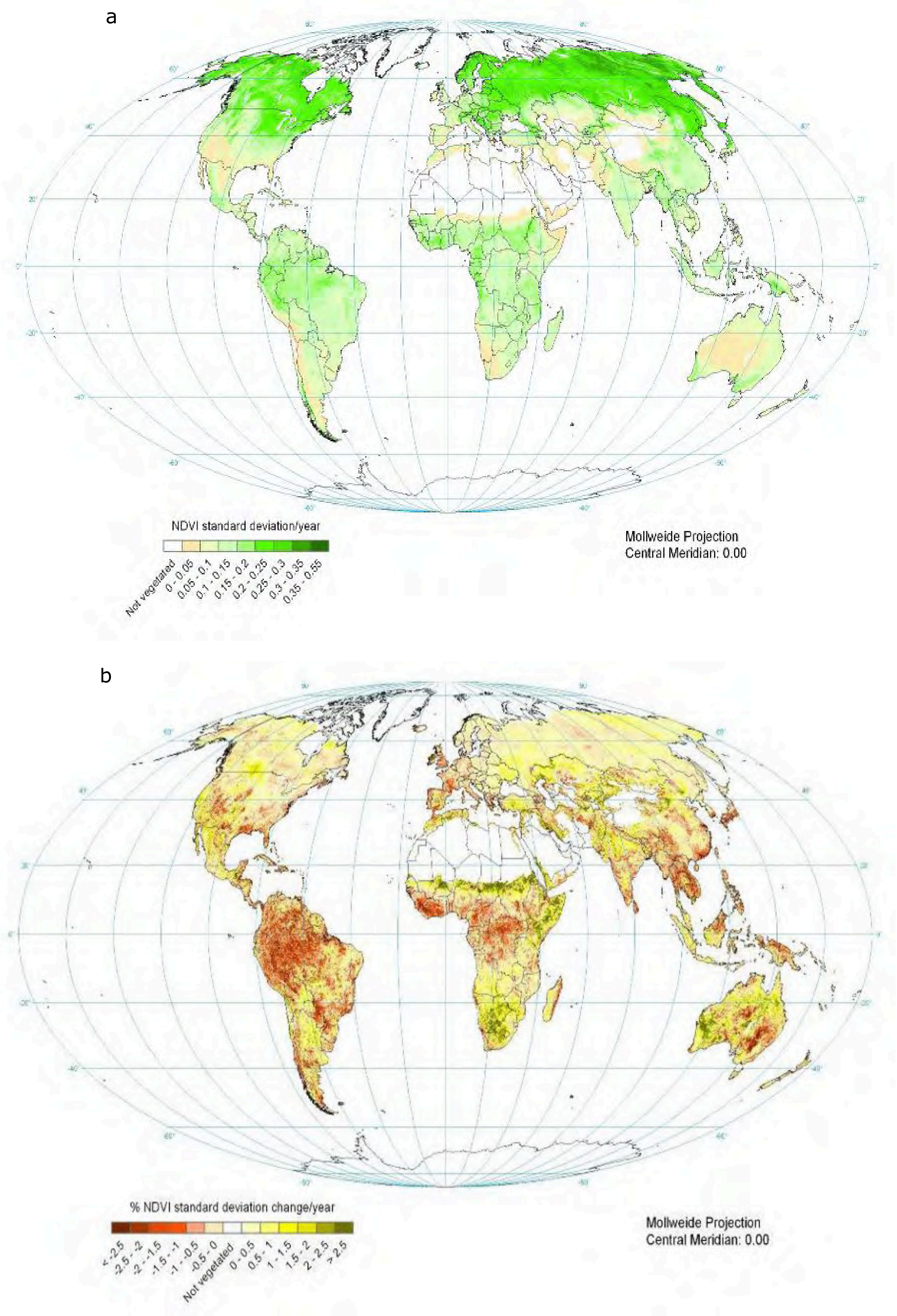

Figure S6. NDVI standard deviation 1981-2003: Pattern (a), trends (b – percentage)

c

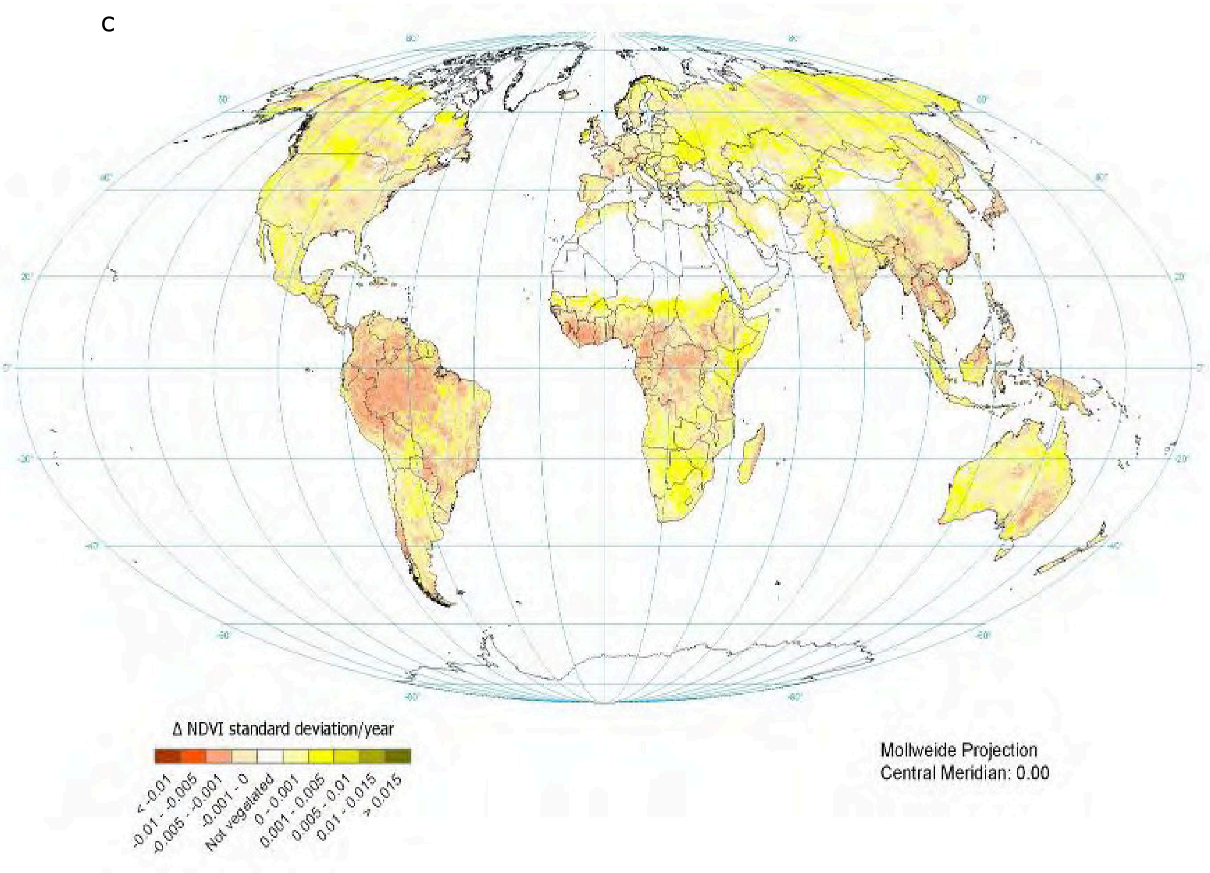

d

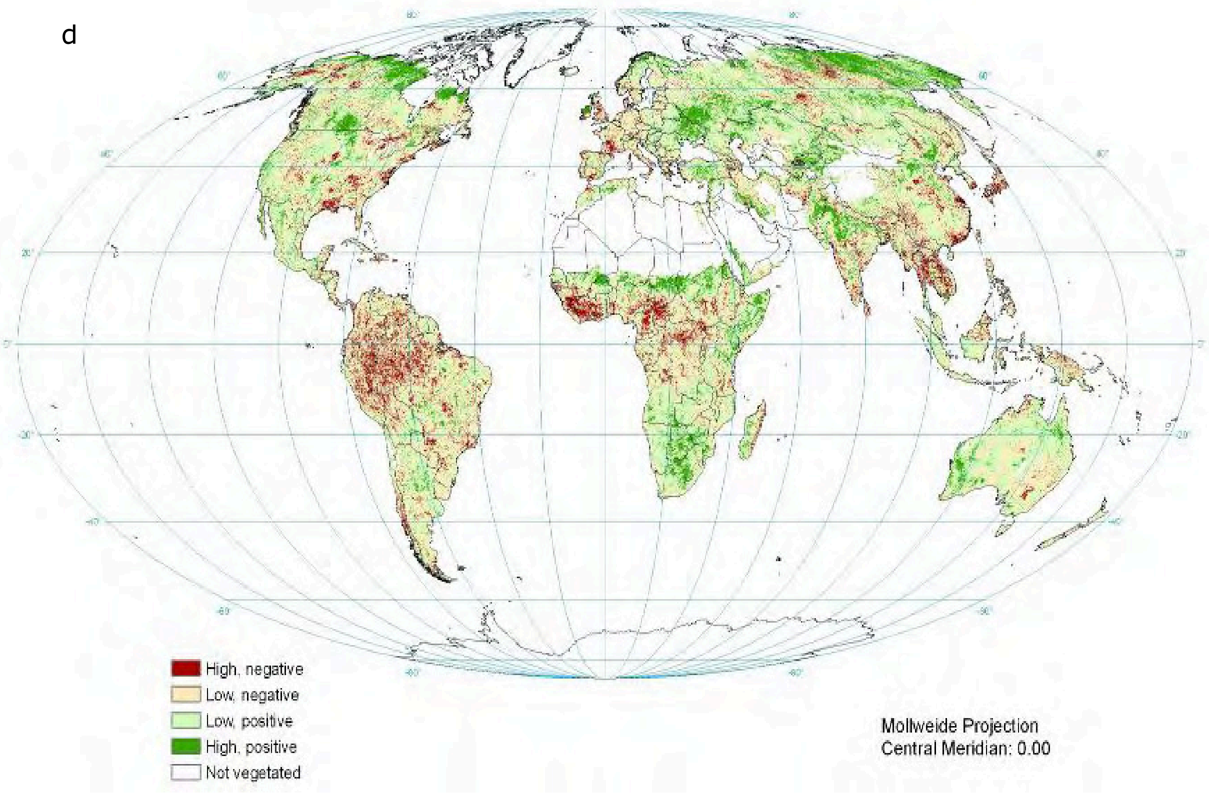

Figure S6. NDVI standard deviation 1981-2003: Trends (c – absolute) and confidence levels (d)

a

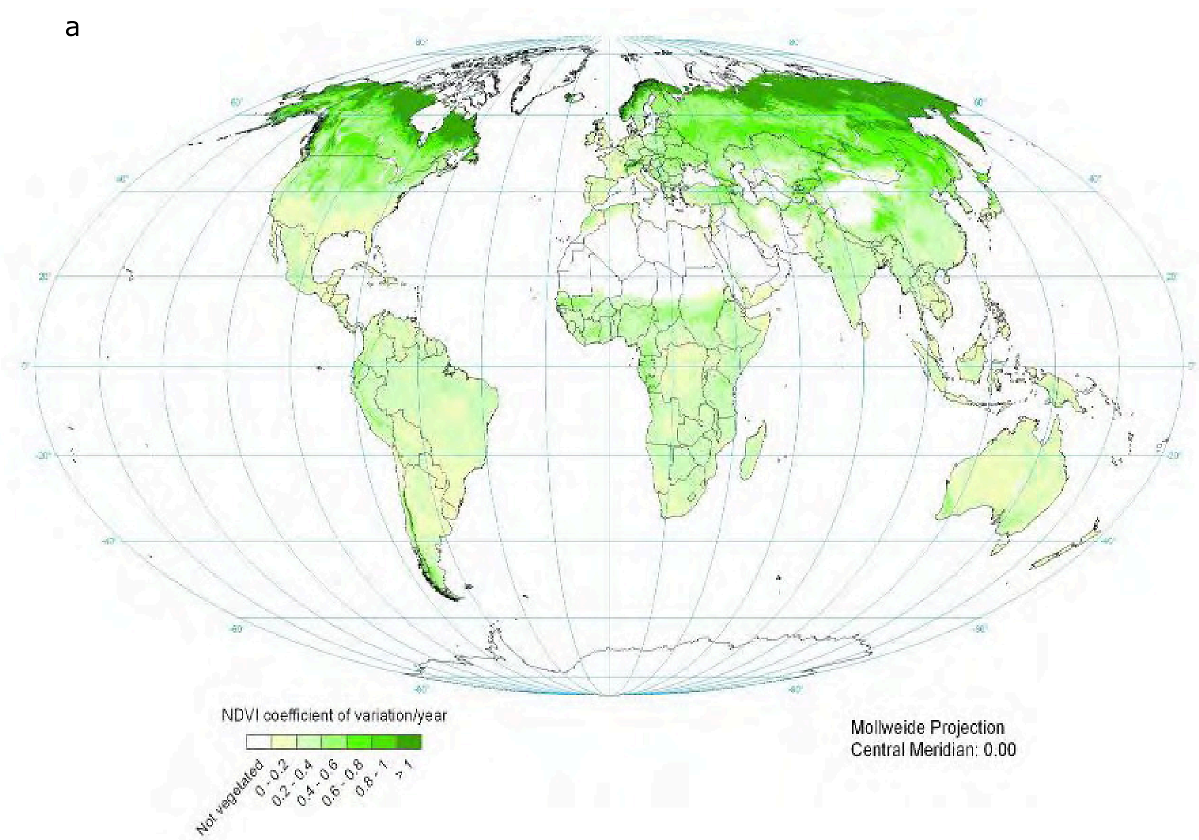

b

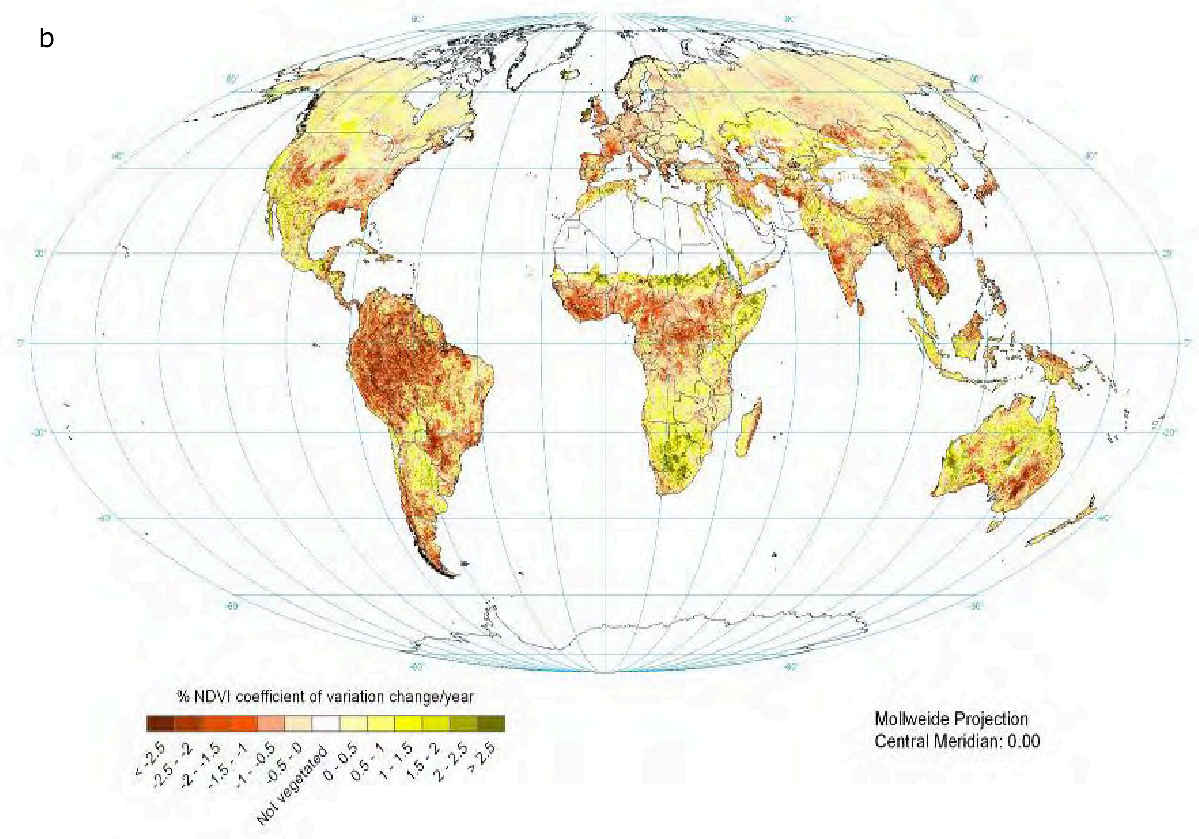

Figure S7. NDVI coefficient of variation 1981-2003: Pattern (a), trends (b – percentage)

c

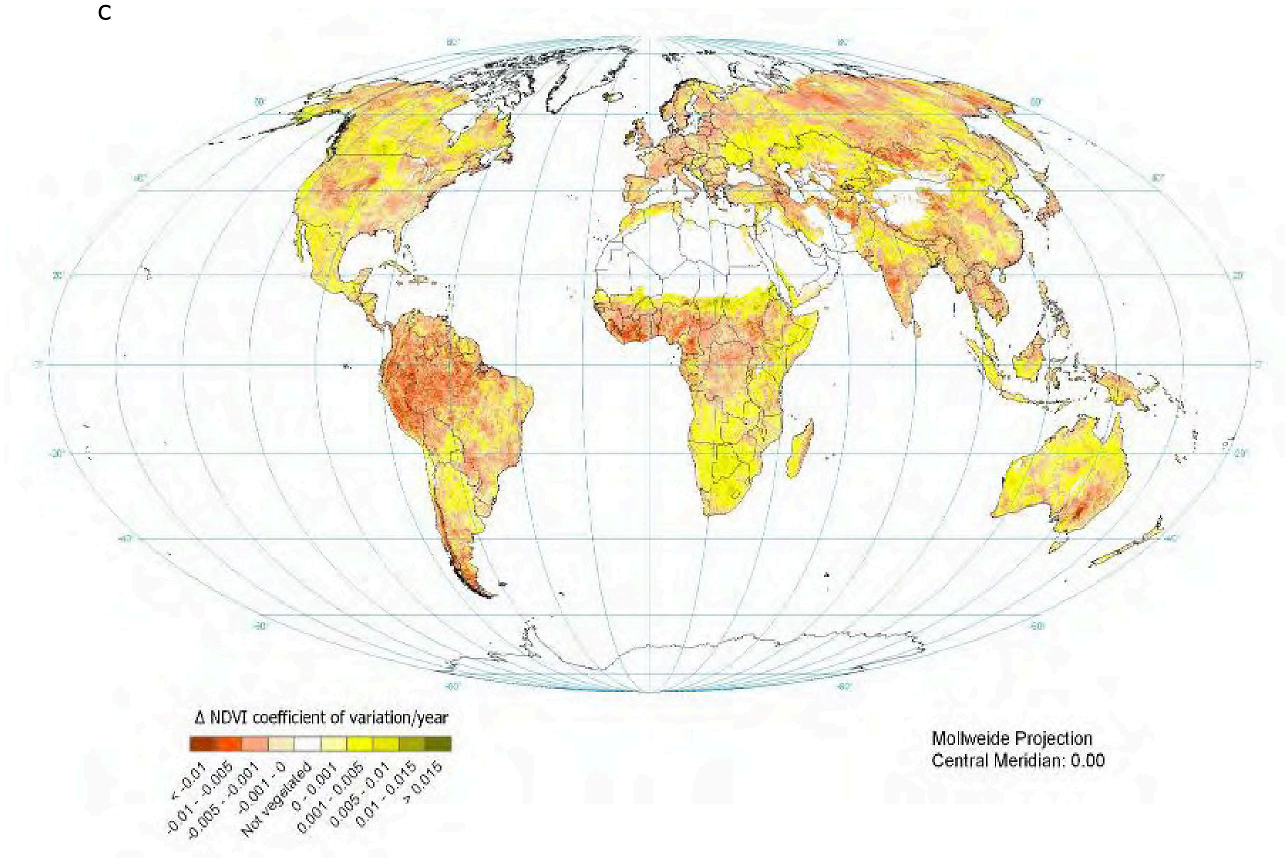

d

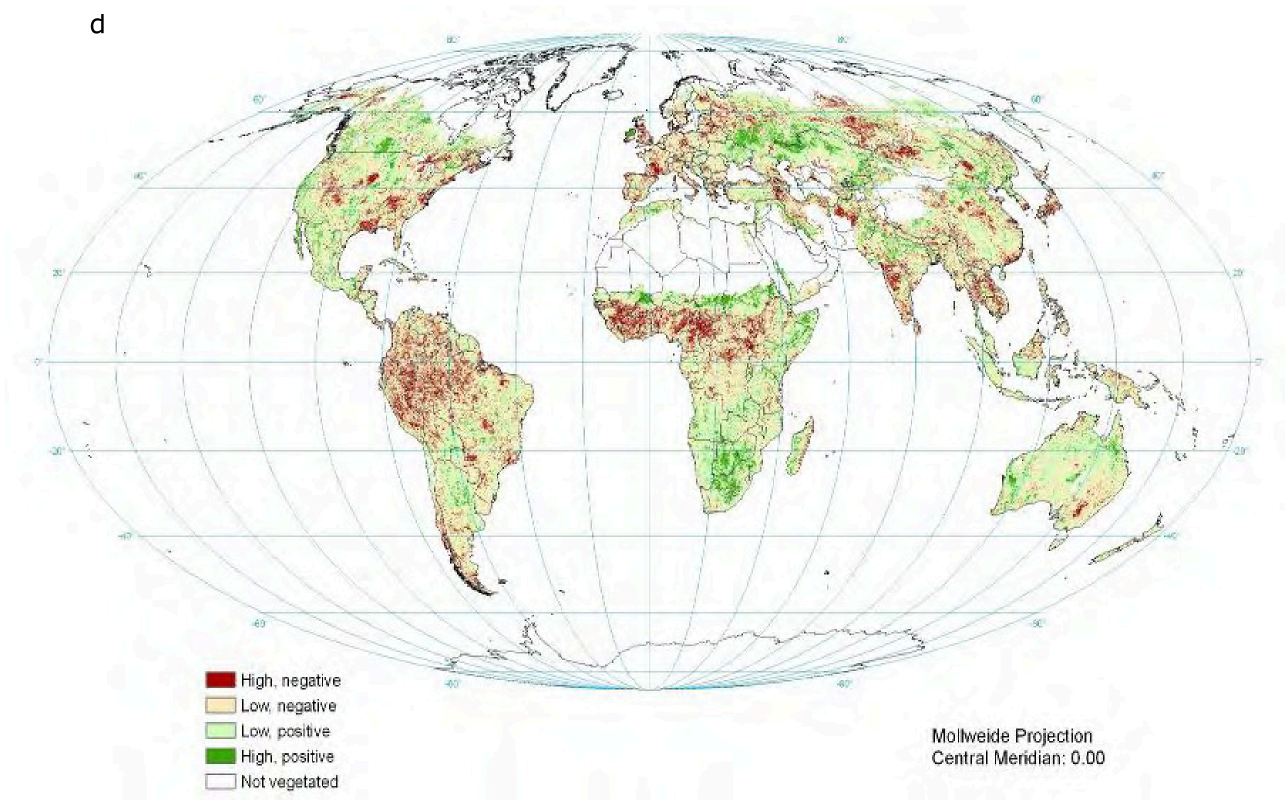

Figure S7. NDVI coefficient of variation 1981-2003: Trends (c – absolute) and confidence (d)